

**NUMERICAL APPROXIMATION OF BLOW-UP  
OF RADially SYMMETRIC SOLUTIONS OF  
THE NONLINEAR SCHRÖDINGER EQUATION**

G.D. Akrivis, V.A. Dougalis,  
O.A. Karakashian, W.R. McKinney

**19-97**

**Preprint no. 19-97/1997**

**Department of Computer Science  
University of Ioannina  
451 10 Ioannina, Greece**

# NUMERICAL APPROXIMATION OF BLOW-UP OF RADIALLY SYMMETRIC SOLUTIONS OF THE NONLINEAR SCHRÖDINGER EQUATION

by

Georgios D. Akrivis<sup>\*</sup>

Vassilios A. Dougalis<sup>†</sup>

Ohannes A. Karakashian<sup>‡</sup>

and

William R. McKinney<sup>§</sup>

December 8, 1997

## Abstract

We consider the initial-value problem for the radially symmetric nonlinear Schrödinger equation with cubic nonlinearity (NLS) in  $d = 2$  and  $3$  space dimensions. To approximate smooth solutions of this problem, we construct and analyze a class of numerical methods based on a standard Galerkin finite element spatial discretization and on suitable implicit Runge-Kutta time-stepping procedures. We then equip one of these schemes with an adaptive, spatial and temporal mesh refinement mechanism that enables the numerical technique to approximate well singular solutions of the NLS that blow up at the origin as the temporal variable  $t$  tends from below to a finite value  $t^*$ . For the blow-up of the amplitude of the solution we recover the well-known rates  $(t^* - t)^{-\frac{1}{2}}$  for  $d = 3$  and  $[\ln \ln \frac{1}{t^* - t} / (t^* - t)]^{1/2}$  for  $d = 2$ . The scheme also approximates well the details of the blow-up of the phase of the solution at the origin as  $t \rightarrow t^*$ .

**Keywords.** Nonlinear Schrödinger equation, point blow-up, finite element methods, adaptive mesh refinement.

**AMS subject classifications:** 65M60, 65M50, 35Q55.

## 1. INTRODUCTION

The nonlinear Schrödinger equation with cubic nonlinearity (henceforth referred to as “NLS equation”) is given by

$$u_t = i\Delta u + i|u|^2 u, \quad x \in \mathbb{R}^d, \quad t \geq 0, \quad (1.1a)$$

---

<sup>\*</sup>Computer Science Department, University of Ioannina, 451 10 Ioannina, Greece.

<sup>†</sup>Mathematics Department, University of Athens, Panepistemiopolis, 157 84 Zographou, Greece, and Institute of Applied and Computational Mathematics, Research Center of Crete, FO.R.T.H., Greece.

<sup>‡</sup>Mathematics Department, University of Tennessee, Knoxville, Tennessee 37996, USA.

<sup>§</sup>Mathematics Department, North Carolina State University, Raleigh, N.C. 27695, USA.

wherein  $u$  is a complex-valued function of the ‘spatial’ variable  $x \in \mathbb{R}^d$ ,  $d = 1, 2, 3$ , and of the ‘temporal’ variable  $t \geq 0$ . The equation occurs frequently in various areas of Mathematical Physics, posed as an initial-value problem with given initial condition

$$u(x, 0) = u^0(x), \quad x \in \mathbb{R}^d. \quad (1.1b)$$

For example, for  $d = 1$  it arises as an envelope equation in water wave theory, [Ne]. In two space dimensions it occurs in nonlinear optics, where it describes in certain regimes the propagation of electromagnetic beams in media whose index or refraction depends on the amplitude of the field in a simple nonlinear way, [CGT], [Ta]. For  $d = 3$  it is obtained as a limiting case of Zakharov’s model of Langmuir waves, [Za]. For a review of various mathematical and physical aspects of the problem (1.1a-b) see [CH], [Str], [RR] and the references therein.

It is not hard to see that for  $d = 1$  the initial-value problem (1.1a-b) is globally well-posed for smooth enough initial data that decays sufficiently fast at infinity. It is also well known that in this case it can be solved by the inverse scattering transform, [Ne]. For  $d = 2, 3$  we have local existence, cf. e.g. [GV], [Ka], and global existence for suitably restricted initial data, [CH], [We]. It is also well known that for  $d \geq 2$  there exist singular solutions which blow up in  $L^\infty$  in finite time, [Gl]. The blow-up in the critical, two-dimensional case is usually referred to as “self-trapping” or “self-focusing”, [CGT], [Ta], whereas the blow-up in the supercritical, three-dimensional case is sometimes referred to as “collapse”, [Za].

In this paper we shall be interested in the numerical approximation of radially symmetric solutions of the initial-valued problem for the NLS in  $d = 2$  and 3 dimensions. We make therefore the hypothesis that the function  $u^0$  in the initial condition (1.1b) and, consequently, the solution of (1.1a) are radially symmetric, i.e., that  $u = u(r, t)$  for  $t \geq 0$ , where  $r = |x| = (x_1^2 + \dots + x_d^2)^{\frac{1}{2}}$ . Hence our problem becomes

$$u_t = i(u_{rr} + \frac{d-1}{r}u_r) + i|u|^2u, \quad r > 0, \quad t \geq 0, \quad (1.2a)$$

$$u_r(0, t) = 0, \quad t \geq 0, \quad (1.2b)$$

$$u(r, 0) = u^0(r), \quad r \geq 0. \quad (1.2c)$$

It is straightforward to check that the  $L^2$  norm and the Hamiltonian of the solution of (1.1a-b) are conserved. In the presence of radial symmetry, i.e. for problem (1.2a-c), these invariants are

$$\int_0^\infty |u(r, t)|^2 r^{d-1} dr = \text{const. for } t \geq 0, \quad (1.3)$$

$$\int_0^\infty \left( |u_r(r, t)|^2 - \frac{1}{2}|u(r, t)|^4 \right) r^{d-1} dr = \text{const. for } t \geq 0. \quad (1.4)$$

In recent years there has appeared a considerable amount of work aimed at describing in detail, by numerical and asymptotic means, the characteristics of the blow-up of solutions of (1.2 a-c) for  $d = 3$  and 2. We refer the reader to a series of publications, [SSP], [McPSS], [LePSS1], [LePSS2], [LPSS], [LePSS3], [LPSSW] of a group including Papanicolaou, C. Sulem, P.L. Sulem and their co-workers. We also refer to the work of the group of Zakharov and his co-workers, which went on for many years and was conveniently summarized in [KSZ]; this paper also contains references to earlier Russian work on the subject. For more recent work in the critical case cf. [Ma], [Fi], [FP].

The main characteristics of the blow-up singularity in the presence of radial symmetry for  $d = 3$  are by now well understood. The problem was studied in [McPSS] by use of a



numerical technique that employs “dynamic rescaling”, a time-dependent change of scales of the solution and the independent variables of (1.2a). The scaling factors are chosen so that suitable functionals of the solution are preserved. It turns out that the transformed dependent variable satisfies a p.d.e. with global solution. This equation is integrated numerically and the details of the blow-up are inferred from the long-time asymptotics of the numerical solution and the scale factors. In this manner, it was concluded in [McPSS] that singular radial solutions in  $d = 3$  dimensions blow up at the origin with an amplitude peak that grows like  $(t^* - t)^{-\frac{1}{2}}$  as  $t$  approaches the blow-up time  $t^* < \infty$ . The computations also provided additional information on the basis of which further conclusions were drawn in [McPSS] on the details of the self-similar structure and the singularity of the phase of the solution as  $t \uparrow t^*$ . Some of these features of the blow-up had been predicted by Zakharov [Za]; see [KSZ] for an account of the largely parallel and analogous work of the Russian school on three-dimensional collapse.

In the two-dimensional case, still for radially symmetric solutions, earlier conclusions in the literature on the blow-up rate of the amplitude, based on numerical and asymptotic computations, varied substantially. This is not surprising;  $d = 2$  is the critical dimension case for the cubic nonlinearity, and the blow-up slows down somewhat, making the numerical integration of the equation harder. Thus, a  $(t^* - t)^{-2/3}$  law for the blow-up of the amplitude was conjectured in [ZS] and [SSP], while  $\left[\ln \frac{1}{t^* - t} / (t^* - t)\right]^{\frac{1}{2}}$  was put forward in [VPT] and [Wo]. It soon became apparent that the amplitude behaved *grosso modo* like  $(t^* - t)^{-\frac{1}{2}}$  but that this behavior was perturbed by a slower varying factor. Using computational (dynamic rescaling) evidence and asymptotic techniques LeMesurier *et al.*, [LePSS1], suggested the form  $F(t^* - t)/(t^* - t)^{\frac{1}{2}}$ , wherein, as  $s \downarrow 0$ ,  $F(s)$  tends to infinity more slowly than  $(\ln \frac{1}{s})^\gamma$  for any  $\gamma > 0$ . Finally, in [LPSS] and [LePSS3] it was concluded that the rate is  $[\ln \ln \frac{1}{t^* - t} / (t^* - t)]^{1/2}$ . This rate had been predicted by Fraiman, [Fr], [SF], on the basis of asymptotic estimates. The Zakharov group favored rates of the form  $[(\ln \frac{1}{t^* - t})^\gamma / (t^* - t)]^{1/2}$  for  $0.35 \leq \gamma \leq 0.65$ , depending on the initial conditions, [KSZ], but estimated that the log log rate probably obtains for  $t$  extremely close to  $t^*$ . The latter conclusion is still maintained in the recent papers [Ma], [Fi], [FP], where new, ‘adiabatic’ rates, which describe accurately the blow-up in its earlier stages and agree asymptotically with the log log law, are proposed.

As an alternative to change of variables and asymptotic techniques one could try to approximate singular solutions of (1.2) by direct numerical integration of the p.d.e. in the  $r, t, u$  variables. In the past such direct numerical simulations were used e.g. in [VPT] (see also the references in [KSZ]), [Wo], [SSP], [TSs]. As the solution blows up, its accurate approximation requires using extremely fine adaptive grids in the spatial variable around the blow-up point, and radically decreasing the time step sizes as  $t$  approaches  $t^*$ . Avoiding the deterioration of the numerical results due to roundoff errors in computing the solution and various quantities of interest derived therefrom (such as blow-up rates), becomes then an overarching consideration, as pointed out by the authors of [KSZ] in their critique of direct integration techniques.

In this paper we shall approximate the solution of (1.2a-b-c) for  $d = 2$  and 3 by an adaptive version of a member of a class of fully discrete numerical schemes based on a Galerkin finite element discretization in the radial variable on a finite interval, coupled with implicit Runge-Kutta time-stepping procedures. In section 2 we address issues of existence, stability and order of convergence of these methods and outline briefly the proofs of the relevant error estimates, which are extensions to the radial case of results that may be found in [ADK1], [KAD], [ADK2]. All our theoretical error estimates hold under the hypotheses that the solution of (1.2) is smooth and the spatial and temporal mesh sizes are fixed. However this will not deter us from proposing suitably adaptive versions of these methods and trying our hand in



approximating with them solutions of the radial problem that blow up at the origin in finite time.

The spatial adaptive technique, described in detail in section 3, consists of a mechanism of reducing automatically the spatial mesh size in the neighborhood of the origin, as the solution steepens, by means of a check on a local  $L^\infty - L^2$  inverse inequality satisfied by members of the finite element subspace. The criterion for cutting the time step is based on controlling a suitably normalized version of the second invariant (Hamiltonian) of the problem. We found that the adaptive mechanism worked well in three as well as two dimensions, allowing numerical solutions to reach maximum values of the ratio  $|u(0, t)|/|u^0(0)|$  of “final” to initial amplitude at the origin of up to  $O(10^{15})$  for  $t$  extremely close to the blow-up time  $t^*$ .

In section 4 we consider the three-dimensional case and report on our numerical computations of rates of blow-up of the amplitude, of various norms of the solution, and of its phase as  $t \rightarrow t^*$ . Paying particular attention to the numerical stability of these rate computations, we verify, using several types of initial profiles, the amplitude blow-up law  $(t^* - t)^{-\frac{1}{2}}$  and reproduce accurately the value of the constant  $\kappa$ , cf. [McPSS], [KSZ], that occurs, e.g., in the formula for the singularity of the phase of the solution, i.e. in the expression  $\exp\left(i\kappa \ln \frac{1}{t^* - t}\right)$  as  $t \rightarrow t^*$ .

In section 5 we turn to the two-dimensional case. We test several laws for the blow-up rate of the amplitude against the results of our numerical simulations for  $t$  extremely close to  $t^*$ . Our conclusion is that the log log rate of [LPSS], [LePSS3], [Fr], provides a highly accurate fit to our data. The description of the phase singularity turns out to be quite a challenging problem in two dimensions, cf. [LPSS]. We were able to confirm that the approximate value of the constant  $\lambda$  occurring e.g. in the expression of the phase of the singular solution at  $r = 0$  (which, to first-order terms, is  $\exp\left(\frac{1}{2\lambda} \ln \frac{1}{t^* - t} \ln \ln \frac{1}{t^* - t}\right)$  according to [LPSS]) is equal to  $\pi$ , something that was predicted on the basis of a “descent” argument from higher dimensions in [LPSS] but not actually seen in numerical simulations of the evolution equation in that work. (That the constant is equal to  $\pi$  can also be predicted by more ‘physical’, asymptotic arguments, cf., e.g., [Ma].)

We close with a section of conclusions and comments on other related research directions. A preliminary report of some of the results of this paper appeared in [ADKMc].

## 2. FULLY DISCRETE GALERKIN METHODS FOR THE RADIAL PROBLEM

In this section we consider the radial problem (1.2) posed on a finite interval  $0 \leq r \leq R$  with zero Dirichlet boundary condition at  $r = R$ , i.e. the initial- and boundary-value problem

$$u_t = i(u_{rr} + \frac{d-1}{r}u_r) + i|u|^2u, \quad 0 \leq r \leq R, \quad 0 \leq t \leq T, \quad (2.1a)$$

$$u_r(0, t) = 0, \quad 0 \leq t \leq T, \quad (2.1b)$$

$$u(R, t) = 0, \quad 0 \leq t \leq T, \quad (2.1c)$$

$$u(r, 0) = u^0(r), \quad 0 \leq r \leq R, \quad (2.1d)$$

where  $d = 2$  or  $3$ . In the sequel we shall denote  $L^p$  norms,  $1 \leq p < \infty$ , of radial functions defined on  $[0, R]$  by

$$\|u\|_{L^p} = \left( \int_0^R |u(r)|^p r^{d-1} dr \right)^{\frac{1}{p}},$$

and put  $\|u\| = \|u\|_{L^2}$ ,  $\|u\|_{L^\infty} = \text{ess sup}_{0 \leq r \leq R} |u(r)|$ . The  $L^2$  inner product  $\int_0^R u(r) \overline{v(r)} r^{d-1} dr$  of two complex-valued radial functions will be denoted by  $(u, v)$ . The solution of the problem (2.1) also conserves the analogs of (1.3) and (1.4) which, in the present context, become for  $0 \leq t \leq T$ :

$$\|u(t)\| = \|u^0\|, \quad (2.2)$$

$$H(u(t)) := \|u_r(t)\|^2 - \frac{1}{2} \|u\|_{L^4}^4 = H(u^0) := \|u_r^0\|^2 - \frac{1}{4} \|u^0\|_{L^4}^4. \quad (2.3)$$

We shall approximate the solution of (2.1) by fully discrete Galerkin-finite element methods that use continuous piecewise polynomial functions in the radial variable; the temporal discretization will be effected by a class of implicit Runge-Kutta schemes. The stability and convergence of such methods have been analyzed in detail in [ADK1] and [KAD] for the NLS in Cartesian coordinates. Although there are several instances where the techniques of the convergence proof in the radial case depart from their counterparts in [KAD], the overall scheme of proof remains basically the same with that of the latter reference. In this section we shall therefore establish notation and state our results without proof, providing where needed some commentary and pointing out differences between the radial and the Cartesian cases. Our theoretical results on the rate of convergence of the methods require that the solution of (2.1) is sufficiently smooth in  $[0, R] \times [0, T]$ , that the radial mesh is quasiuniform and the time step is constant. However, in subsequent sections we shall use adaptive versions of our base scheme to approximate the singular solutions as they blow up. This will require drastic local refinement of the radial mesh and fast reduction of the temporal step to extremely small values. There is as yet no satisfactory convergence theory available for such adaptive schemes.

Let  $0 = r_0 < r_1 < \dots < r_N = R$  be a quasiuniform partition of  $[0, R]$  with  $h = \max_i (r_i - r_{i-1})$ . For integer  $s \geq 2$  let  $S_h^s$  be the space of complex-valued continuous functions on  $[0, R]$  that vanish at  $r = R$  and are polynomials of degree at most  $s - 1$  on each interval  $(r_{i-1}, r_i)$ ,  $1 \leq i \leq N$ . We seek first a semidiscrete approximation  $u_h(r, t) \in S_h^s$  to  $u(r, t)$  for each  $t \in [0, T]$ . This is defined in the customary way as a map  $u_h : [0, T] \rightarrow S_h^s$  satisfying the equations

$$(u_{ht}, \chi) + ia(u_h, \chi) = i(|u_h|^2 u_h, \chi) \quad \forall \chi \in S_h^s, \quad 0 \leq t \leq T, \quad (2.4a)$$

$$u_h(0) = u_h^0, \quad (2.4b)$$

where  $a(u, v) = \int_0^R r^{d-1} u_r \overline{v_r} dr$ , and  $u_h^0$  is chosen so that

$$\|u^0 - u_h^0\| \leq ch^s. \quad (2.5)$$

For example,  $u_h^0$  could be the  $L^2$  projection of  $u^0$  onto  $S_h^s$ . In (2.5) and in the sequel the generic  $c$  will denote positive constants independent of the discretization parameters but possibly depending on the solution of (2.1). Note that the condition  $u_r(0, t) = 0$  is not imposed on the subspace and disappears from the variational formulation. It is not hard to see that the solution  $u_h(t)$  of the system of ordinary differential equations represented by (2.4) exists at least locally and satisfies the discrete analogs of the conservation laws (2.2) and (2.3).

To estimate the error  $u_h - u$  we define the *elliptic projection*  $P_E w$  of a function  $w$  of the space  $\dot{H}^1$ , the set of continuous radial functions on  $(0, R]$  that vanish at  $x = R$  and satisfy  $\|w_r\| < \infty$ , as the map  $P_E : \dot{H}^1 \rightarrow S_h^s$  satisfying

$$a(P_E w, \chi) = a(w, \chi) \quad \forall \chi \in S_h^s.$$

It may be seen, cf. [ETH], [SE], that  $P_E w$  exists uniquely and satisfies

$$\|w - P_E w\| \leq ch^s \|w^{(s)}\|, \quad (2.6)$$



where  $w^{(s)}$  denotes the  $s^{\text{th}}$  (radial) derivative of  $w$ . It should be noted that for Lagrangian finite element spaces an interpolant is constructed in [TSsM] that permits proving (2.6) for general, i.e. not necessarily quasiuniform, meshes. However the quasiuniformity assumption expedites the error estimation (especially in the convergence theory of the fully discrete approximations to follow) in that it implies the inverse inequality

$$\|v_h\|_{L^\infty} \leq ch^{-\frac{d}{2}} \|v_h\| \quad \text{for } v_h \in S_h^s, \quad (2.7)$$

that will be used in the error estimates to follow.

Arguing now along the lines of the proof of Theorem 2.1 of [ADK1], we compare the semidiscrete approximation  $u_h$  to the solution of a perturbed semidiscretization of (2.1) that is defined by replacing the nonlinear term in the right-hand side of (2.4a) by a suitably cut-off globally Lipschitz approximation thereof. Using (2.7) and the properties of the elliptic projection operator, we may then prove the following  $L^2$  optimal rate of convergence error estimate.

**Theorem 2.1** *Suppose  $u$ , the solution of (2.1), is sufficiently smooth on  $[0, R] \times [0, T]$ . Then, if  $u_h^0$  satisfies (2.5) the solution  $u_h(t)$  of (2.4a,b) exists uniquely in  $S_h^s$  for  $0 \leq t \leq T$ . Moreover, there exists a constant  $c$  such that*

$$\max_{0 \leq t \leq T} \|u(t) - u_h(t)\| \leq ch^s. \quad (2.8)$$

□

(It should be noted that in [TSsM], an error estimate like (2.8) is established for Lagrange-type finite element spaces under the assumption that  $h \leq C(\min_i(r_i - r_{i-1}))^\theta$ , where  $\theta$  is any number in  $(0, 1)$ .)

We turn now to temporal discretizations of (2.4). For this purpose we shall use implicit Runge-Kutta methods because of their favorable stability properties and high order of accuracy. Let  $k$  be the (constant in this section) time step and let  $t^n = nk$ ,  $n = 0, 1, 2, \dots, J$ ,  $Jk = T$ . For  $q \geq 1$ , a  $q$ -stage Implicit Runge-Kutta (IRK) method is defined by a set of  $q^2 + 2q$  real constants, [Bu], arranged as elements of a  $q \times q$  matrix  $A = (a_{ij})$  and two vectors  $(b_1, \dots, b_q)^T$  and  $(\tau_1, \dots, \tau_q)^T$ . Given the initial-value problem  $dy/dt = f(t, y)$ ,  $0 \leq t \leq T$ ,  $y(0) = y^0$ , the IRK methods generate approximations  $y^n$  to  $y(t^n)$  by the formulas

$$\begin{aligned} y^{n,j} &= y^n + k \sum_{m=1}^q a_{jm} f(t^{n,m}, y^{n,m}), \quad 1 \leq j \leq q, \\ t^{n,j} &= t^n + \tau_j k, \quad 1 \leq j \leq q, \\ y^{n+1} &= y^n + k \sum_{j=1}^q b_j f(t^{n,j}, y^{n,j}). \end{aligned} \quad (2.9)$$

We shall assume that these methods satisfy certain stability and accuracy conditions. In particular, we require that the methods be *algebraically stable*, [Bu], i.e. that  $b_i \geq 0$ ,  $1 \leq i \leq q$ , and that the  $q \times q$  matrix with elements  $m_{ij} := a_{ij}b_i + a_{ji}b_i - b_i b_j$  is positive semidefinite. The accuracy conditions that we shall assume to hold are known as *simplifying assumptions*, [Bu], and state that there exist integers  $\nu, p, \rho \geq 1$  with  $\nu \leq p + \rho + 1$ ,  $\nu \leq 2p + 2$  such that

$$\sum_{j=1}^q b_j \tau_j^\ell = \frac{1}{\ell + 1}, \quad 0 \leq \ell \leq \nu - 1,$$

$$\sum_{j=1}^q a_{ij} \tau_j^\ell = \frac{\tau_i^{\ell+1}}{\ell+1}, \quad 1 \leq i \leq q, \quad 0 \leq \ell \leq p-1,$$

$$\sum_{i=1}^q a_{ij} \tau_i^\ell b_i = \frac{b_j}{\ell+1} (1 - \tau_j^{\ell+1}), \quad 1 \leq j \leq q, \quad 0 \leq \ell \leq \rho-1.$$

We shall refer to  $p$  and  $\nu$  as the *stage order*, and the *classical order*, respectively, of the IRK method. The simplifying assumptions imply that for smooth  $f$ , we have  $y(t^n) - y^n = O(k^\nu)$ , i.e. that the error decreases at a rate equal to the classical order. Finally, *existence* of solutions of the  $q \times q$  nonlinear system defining the intermediate stages  $y^{n,j}$  will follow for our problem if we assume a *positivity* property [DV], [CHS], namely that the matrix  $A = (a_{ij})$  is invertible and there exists a  $q \times q$  positive diagonal matrix  $D$  such that  $DA^{-1}D^{-1}$  is positive definite. The class of IRK schemes that satisfy the above properties includes the Gauss-Legendre methods, for which  $\nu = 2q$ ,  $p = \rho = q$ , the Radau IIA methods (with  $\nu = 2q - 1$ ,  $p = q$ ,  $\rho = q - 1$ ), etc. For other examples and further remarks cf. [KAD]. It should be added that the Gauss-Legendre schemes are *conservative* in the sense that they satisfy  $m_{ij} = 0$ , where  $m_{ij}$  are the entries of the matrix intervening in the definition of algebraic stability. This property will imply that our fully discrete approximations, to be defined presently, are conservative in the  $L^2$  sense.

Applying now the IRK method (2.9) to the semidiscrete system (2.4) yields our base time-stepping scheme as follows: Let  $U^n \in S_h^s$  be the fully discrete approximation to  $u_h(t^n)$  (or  $u(x, t^n)$ ). Then, an approximation  $U^{n+1}$  to  $u_h(t^{n+1})$  is computed in terms of  $q$  functions  $U^{n,j} \in S_h^s$ ,  $1 \leq j \leq q$ , the intermediate stages of the scheme, according to

$$u^0 = u_h^0, \quad (2.10a)$$

for  $n = 0, 1, 2, \dots, J-1$ :

$$U^{n,j} = U^n + k \sum_{m=1}^q a_{jm} f_h(U^{n,m}), \quad 1 \leq j \leq q, \quad (2.10b)$$

$$U^{n+1} = U^n + k \sum_{j=1}^q b_j f_h(U^{n,j}). \quad (2.10c)$$

In these formulas we have put  $f_h = i(\Delta_h + g_h)$ , where  $\Delta_h, g_h : S_h^s \rightarrow S_h^s$  are, respectively, the approximation of the Laplacian in radial coordinates and the nonlinear map, defined for  $\varphi \in S_h^s$  by  $(\Delta_h \varphi, \chi) = a(\varphi, \chi)$ ,  $(g_h(\varphi), \chi) = (|\varphi|^2 \varphi, \chi) \quad \forall \chi \in S_h$ .

Existence of solutions of the nonlinear system represented by (2.10b) can be proved (entirely analogously to the argument in Proposition 3.1 of [KAD]) using the Brouwer fixed point theorem and the ‘positivity’ property of the IRK method. In addition, as a consequence of the algebraic stability of the scheme, we may prove, essentially as in Proposition 3.2 of [KAD], that the solutions of (2.10) satisfy

$$\|U^{n+1}\| \leq \|U^n\|, \quad n = 0, 1, \dots, J-1, \quad (2.11)$$

in the radial case as well. Indeed, for conservative methods such as the Gauss-Legendre, (2.11) is an equality.

We turn now to estimating the error  $u(t^n) - U^n$  in the  $L^2$  norm. It is well known that approximating smooth solutions of initial- and boundary-value problems of some p.d.e.’s by high order Runge-Kutta methods results sometimes in observed temporal rates of convergence



lower than the classical order  $\nu$ , cf. e.g. [Cr], [DV], [CBT]. It was shown in [KAD] that if  $\Omega$  is a bounded domain with smooth boundary in  $\mathbb{R}^d$  and we consider the initial- and boundary-value problem for the NLS in  $\Omega$  with Dirichlet boundary conditions on  $\partial\Omega$  assuming that  $u$  is smooth on  $\bar{\Omega} \times [0, T]$  and certain weak conditions on the discretization parameters, then the  $L^2(\Omega)$  norm of  $u(t^n) - U^n$  can be bounded by a quantity of  $O(k^\sigma + h^s)$ , where

$$\sigma = \min(p + 3, \nu). \quad (2.12)$$

In particular, no reduction of the classical order  $\nu$  occurs if  $\nu \leq p + 3$ , as is the case with the practically important  $q$ -stage Gauss-Legendre methods of up to three stages. In the special case of a polyhedral domain in  $\mathbb{R}^d$  (interval for  $d = 1$ ) (2.12) is replaced by  $\sigma = \nu$ , i.e. the classical order is recovered. In the study of the temporal order of accuracy of these methods, a key role is played by the degree of compatibility of the solution with the homogeneous boundary condition on  $\partial\Omega$ , cf. [KAD].

In the radial case, although the problem is univariate in space, we can only prove that the temporal component of the error decreases at the rate  $\sigma$  given by (2.12). As in section 4 of [KAD], the proof requires the introduction of certain smooth functions  $\alpha_{j\ell}(r)$ ,  $1 \leq j \leq q$ ,  $0 \leq \ell \leq \nu$ , defined on  $[0, R]$  by the radial analogs of formulas (4.1) of [KAD]. The key idea is then to show that  $\alpha_{j\ell}(R) = 0$  for  $1 \leq j \leq q$ ,  $0 \leq \ell \leq \sigma$ , with  $\sigma$  as high as possible. We can prove that in general  $\sigma = \min(p + 3, \nu)$ . A long series of computations following the general scheme of proof of [KAD] finally yields the following result.

**Theorem 2.2** *Suppose that the solution  $u$  of (2.1) is sufficiently smooth on  $[0, R] \times [0, T]$ . Then, if  $U^0 = u_h^0$  satisfies (2.5) there exists a unique solution  $\{U^n\}_{n=0}^J$  of the fully discrete scheme (2.10) satisfying*

$$\max_{0 \leq n \leq J} \|u(t^n) - U^n\| \leq c(k^\sigma + h^s), \quad (2.13)$$

with  $\sigma$  given by (2.12), provided  $k$  is sufficiently small, that  $s > d/2$  and that  $k = o(h^{d/2\sigma})$  as  $h \rightarrow 0$ .  $\square$

Of course, whenever an IRK method is used to generate approximations to nonlinear evolution equations, there arises the issue of solving, at each time step, the nonlinear system that defines the intermediate stages. In our case this is the  $q \dim S_h^s \times q \dim S_h^s$  nonlinear system represented by (2.10b), whose solution is  $\{U^{n,j}\}$ ,  $1 \leq j \leq q$ . This system must be solved efficiently since almost all the computational work in each time step is concentrated there.

The numerical solution of (2.10b) involves approximating  $U^{n,j}$  for each  $0 \leq n \leq J - 1$  and  $1 \leq j \leq q$  by a sequence of iterates  $U_\ell^{n,j}$ ,  $\ell = 1, \dots, \ell_n$ ,  $\ell_n \geq 1$ . Starting values  $U_0^{n,j}$  for the iteration may be obtained by extrapolation from previously computed steps. To generate the  $U_\ell^{n,j}$  one may use Newton's method or modified versions thereof; cf. [ADK1], [ADK2] for the relevant analysis. Here we adopt a much simpler iterative scheme, a so-called "explicit-implicit" method in which the terms  $f_h(U^{n,m})$  in (2.10b) are split into their linear  $i\Delta_h U^{n,m}$  and nonlinear part  $ig_h(U^{n,m})$ , that are evaluated at the iteration levels  $\ell+1$  and  $\ell$ , respectively. The iterative scheme for the approximation of the  $U^{n,j}$  then becomes: Given  $U^n$ ,  $U_0^{n,j}$  for  $1 \leq j \leq q$ , solve for  $U_\ell^{n,j}$  for  $1 \leq j \leq q$  by

$$U_{\ell+1}^{n,j} - ik \sum_{m=1}^q a_{jm} \Delta_h U_{\ell+1}^{n,m} = U^n + ik \sum_{m=1}^q a_{jm} g_h(U_\ell^{n,m}), \quad \ell = 0, 1, \dots, \ell_n - 1. \quad (2.14)$$

The approximation  $U^{n+1}$  is finally defined by (2.10c) by replacing The approximation  $U^{n+1}$  is finally defined by (2.10c) by replacing  $U^{n,j}$  by their final approximations  $U_{\ell_n}^{n,j}$ . Implementing

(2.14) requires, at each time step  $t^n$ , solving systems with the linear operator  $I - ikA\Delta_h$  on  $(S_h^s)^q$ . This system, if  $k$  is constant, has a matrix independent of  $n$  and  $\ell$ . Moreover, in many cases it may decouple into  $q$  independent subsystems of size  $\dim S_h \times \dim S_h$ , [ADK2]. In the Cartesian variable case (we expect the proof to be entirely analogous in the radial case) the following were shown in [ADK2]: Let  $\sigma$  be given by (2.12) and put  $\bar{p} = \min(p, \sigma - 1)$ . For  $0 \leq j \leq \bar{p}$  choose initial values  $U^j$  that approximate  $u(t^j)$  in  $L^2$  to  $O(k^\sigma + h^s)$  accuracy. This may be done in a variety of ways, cf. [ADK2]. At each time step  $n \geq \bar{p}$ , compute starting values  $U_0^{n,j}$  for the iteration (2.14) by a  $\bar{p}^{\text{th}}$  degree polynomial extrapolation from previous values  $U^{n-j}, 0 \leq j \leq \bar{p}$ . Then, provided  $s > \frac{d}{2}$  and that  $k^{\bar{p}+1}h^{-d/2}$  is sufficiently small, performing  $\ell_n = \sigma - \bar{p} + 1$  iterations in (2.14) will yield an overall stable scheme and produce approximations  $U^n$  to  $u(t^n)$  for which the  $L^2$  error estimate (2.13) continues to hold. For example, in the case of the 1-stage Gauss-Legendre scheme (the midpoint method) for which  $p = 1, \nu = 2$ , we see that taking  $\bar{p} = 1$  and  $\ell_n = 2$  will yield an overall stable fully discrete scheme with an  $O(k^2 + h^s)$   $L^2$  error bound provided  $s > d/2$  and  $k = o(h^{d/4})$ . In the case of the 2-stage Gauss-Legendre scheme (the (2, 2) Padé method) we have  $p = 2, \nu = 4$ . Here  $\bar{p} = 2$ , and taking  $\ell_n = 3, k = o(h^{d/6}), s > d/2$  will give a stable scheme of  $O(k^4 + h^s)$  accuracy in  $L^2$ .

### 3. ADAPTIVE MESH REFINEMENT FOR THE APPROXIMATION OF BLOW-UP

In this section we shall describe the adaptive mechanism that we used to follow the development of a point blow-up singularity of a radially symmetric solution of the initial-value problem of the NLS in  $d = 2$  and 3 dimensions. We shall choose a simple base scheme among those analyzed in the previous section. To normalize matters, we shall scale the radial variable in the initial- and boundary-value problem (2.1) so that it takes values between zero and one. To that effect, scaling  $r \leftarrow r/R$ , we see that (2.1a, b, c, d) become

$$u_t = i\varepsilon(u_{rr} + \frac{d-1}{r}u_r) + i|u|^2u, \quad (r, t) \in (0, 1] \times [0, T], \quad (3.1a)$$

$$u_r(0, t) = 0, \quad 0 \leq t \leq T, \quad (3.1b)$$

$$u(1, t) = 0, \quad 0 \leq t \leq T, \quad (3.1c)$$

$$u(r, 0) = v(r), \quad 0 \leq r \leq 1, \quad (3.1d)$$

where  $\varepsilon = 1/R^2$  and  $v(x) = u^0(xR)$ ,  $0 \leq x \leq 1$ . The invariants for this problem are

$$\int_0^1 |u(r, t)|^2 r^{d-1} dr = \int_0^1 |v(r)|^2 r^{d-1} dr, \quad (3.2)$$

and

$$\begin{aligned} H(u(t)) &:= \int_0^1 (\varepsilon|u_r(r, t)|^2 - \frac{1}{2}|u(r, t)|^4) r^{d-1} dr \\ &= \int_0^1 (\varepsilon|v_r(r)|^2 - \frac{1}{2}|v(r)|^4) r^{d-1} dr =: H(v), \end{aligned} \quad (3.3)$$

for  $0 \leq t \leq T$ .

As we will be mainly interested in describing the evolution of profiles that focus (collapse) fast at  $r = 0$ , (3.1) will furnish a reasonable approximation to (1.2) for large  $R$  and initial data  $u^0$  that decay exponentially, say, with  $r$ .



As our base scheme for approximating the solution of (3.1) we shall use the simplest member of the IRK Gauss-Legendre family, namely the 1-stage midpoint rule corresponding to the parameters  $p = q = \rho = 1$ ,  $\nu = 2$ ,  $a_{11} = \tau_1 = \frac{1}{2}$ ,  $b_1 = 1$ .  $S_h := S_h^2$  will consist of the continuous, complex-valued functions on  $[0, 1]$  that vanish at  $r = 1$  and are piecewise linear relative to an arbitrary partition  $0 = r_0 < r_1 < \dots < r_N = 1$ . The fully discrete scheme amounts then to computing  $\{U^n\} \in S_h$  satisfying for  $n = 0, 1, \dots, J-1$  and all  $\chi \in S_h$

$$\begin{aligned} & \int_0^1 (U^{n+1} - U^n) \bar{\chi} r^{d-1} dr + ik\varepsilon \int_0^1 \left( \frac{U^{n+1} + U^n}{2} \right)_r \bar{\chi} r^{d-1} dr \\ & = ik \int_0^1 \left| \frac{U^{n+1} + U^n}{2} \right|^2 \left( \frac{U^{n+1} + U^n}{2} \right) \bar{\chi} r^{d-1} dr, \end{aligned} \quad (3.4)$$

where  $U^0$  is taken to be the  $L^2$  projection of  $v$  on  $S_h$ . In (3.4) we solve for  $U^* = \frac{1}{2}(U^{n+1} + U^n)$  from the equation

$$\begin{aligned} & \int_0^1 U^* \bar{\chi} r^{d-1} dr + ik\varepsilon \int_0^1 U_r^* \bar{\chi} r^{d-1} dr \\ & = ik \int_0^1 |U^*|^2 U^* \bar{\chi} r^{d-1} dr + \int_0^1 U^n \bar{\chi} r^{d-1} dr \quad \forall \chi \in S_h, \end{aligned} \quad (3.4')$$

and then compute  $U^{n+1} = 2U^* - U^n$ . On each interval Gauss numerical quadrature of sufficient high accuracy is used so that radial polynomials of degree  $d + 3$  are integrated exactly. The nonlinear system implied by (3.4') is solved by explicit-implicit iteration as outlined in the previous section with  $U_0^* = \frac{3}{2}U^n - \frac{1}{2}U^{n-1}$  as starting value for  $n \geq 1$ . Two iterations are performed at each time step except at the first one where three are needed to compensate for the less accurate starting value  $U_0^* = U^0$ . The tridiagonal complex systems attendant are solved by the appropriate Linpack subroutine.

The resulting fully discrete scheme is no longer conservative since the nonlinear system is not solved exactly. However, we found that the  $L^2$  norm of  $U^n$  was conserved to a high degree of accuracy in all our examples, even when  $t$  got very close to the instance of blow-up.

Anticipating that the solution blows up at  $r = 0$  as  $t$  approaches a finite value  $t^*$ , we implemented (3.4) in an adaptive code using a spatial and temporal mesh that can change with  $n$ . (In constructing these adaptive schemes we were aided by experience gained in approximating singular solutions of the generalized Korteweg-de Vries equation, [BDKMc].) As the blow-up time is approached and the solution grows in amplitude near the origin, the adaptive mechanism refines drastically the spatial mesh in a neighborhood of  $r = 0$  and cuts the time step by enforcing two refinement criteria that appeared to be successful for the problem at hand and will be described presently.

If the spatial mesh must be refined, then the number of nodes  $r_i$  is increased as follows: Suppose that the spatial grid has already been refined NSPLIT times. Then,  $[0, 1]$  is partitioned in NSPLIT + 2 adjacent successive intervals  $I_0, I_1, \dots, I_{\text{NSPLIT}+1}$  such that the left-hand boundary of  $I_0$  is 0, the right-hand boundary of  $I_{\text{NSPLIT}+1}$  is 1, and, on each  $I_j$  the mesh is uniform. Specifically, if  $N$  and  $M < 2N$  are given integers and  $h = 1/N$  is the initial spatial meshlength, then:

- $I_0$  consists of  $M$  subintervals of constant meshlength  $h/2^{\text{NSPLIT}+1}$ .
- $I_1$  consists of  $\frac{M}{2}$  subintervals of constant meshlength  $h/2^{\text{NSPLIT}}$ .
- $I_2$  consists of  $\frac{M}{2}$  subintervals of constant meshlength  $h/2^{\text{NSPLIT}-1}$ .

⋮



$I_{\text{NSPLIT}}$  consists of  $\frac{M}{2}$  subintervals of constant meshlength  $h/2$ .  
 $I_{\text{NSPLIT}+1}$  consists of  $N - \frac{M}{2}$  subintervals of constant meshlength  $h$ .

As an example, starting with  $N = 1600$  subintervals, i.e. an initial meshlength  $h = 1/1600 = 0.625 \times 10^{-3}$ , supposing that the finest mesh region always has  $M = 200$  subintervals and assuming that the spatial grid has been refined  $\text{NSPLIT} = 34$  times, we end up with a grid consisting of  $N + \frac{M}{2}(\text{NSPLIT} + 1) = 5100$  subintervals. The coarsest mesh region  $I_{35}$  has 1500 subintervals of width  $h = 0.625 \times 10^{-3}$ , whilst the finest mesh region  $I_0 = (0, r_1)$  consists of 200 subintervals of width  $h/2^{35} \cong 0.182 \times 10^{-15}$ . Each time the grid is refined  $I_0$  is cut in half into two new intervals that are labeled  $I_0$  and  $I_1$ , and all other regions are redefined so that  $I_1$  becomes  $I_2$ ,  $I_2$  becomes  $I_3$ , etc..  $U^n$  is imbedded in the new mesh by linear interpolation.

The signal to perform this spatial grid refinement (i.e. to increase  $\text{NSPLIT}$  by 1) at a certain time step  $n$  is given whenever

$$\frac{\|U^n\|_{L^\infty(I_0)} h_{\min}^{1/2}}{\left(\int_{I_0} |U^n|^2 dr\right)^{\frac{1}{2}}} > \text{TOL}_h. \quad (3.5)$$

Here  $\text{TOL}_h$  is an empirically determined tolerance, usually taken to be equal to 0.12 for  $d = 2$  and from 0.12 to 0.14 for  $d = 3$ , and  $h_{\min}$  is the gridsize on  $I_0$ , which is the interval of finest mesh. The criterion (3.5) is motivated by a local  $L^\infty - L^2$  inverse property that elements of the finite element subspace satisfy on  $I_0$ . The inverse property shows that the growth of the  $L^\infty$  norm is limited by the size of  $h_{\min}$  and the  $L^2$  norm of the solution on  $I_0$  which, close to blow-up, is not changing rapidly. Hence, refining the mesh in the vicinity of  $r = 0$  to satisfy (3.5), allows the amplitude of the solution to grow there.

The time step reduction is motivated by a need to control, to a certain degree, changes in a scaled version of the second invariant of the problem from one time step to the next. Specifically, the time step size  $k$  is halved and the time step computation is repeated whenever

$$\frac{H(U^{n+1}) - H(U^n)}{\int_0^1 |U_r^{n+1}|^2 r^{d-1} dr} > \text{TOL}_k/2. \quad (3.6)$$

In (3.6)  $H(\cdot)$  is the Hamiltonian defined by (3.3) and  $\text{TOL}_k$  is an empirically chosen parameter with values that range from  $10^{-5}$  to  $10^{-8}$ . These values for  $\text{TOL}_k$  and  $\text{TOL}_h$  proved successful in causing the adaptive mechanism to reduce the time step size and refine the spatial grid as needed to simulate accurately the development of the blow-up.

In the three sections that follow we report on the numerical results that we obtained approximating various quantities of interest associated with the singular solutions of the NLS equation in 2 and 3 dimensions. These quantities include rates of growth of the amplitude and of various norms of the solution and its radial derivative, as well as rates of blow-up of the phase of the solution as  $t \rightarrow t^*$ . With this purpose in mind and with the forethought that exceedingly large quantities will develop and their rapid evolution will have to be followed over extremely small temporal increments, we have coded our methods carefully so as to minimize the effect of roundoff errors and maintain stability in the floating point arithmetic. Evidence of that is the ‘stability’ and robustness of most of the blow-up rate output to be presented in the sequel. It should be pointed out that, as a rule, the approximate values of the various rates appear quite early in the computations, before the solution has risen to great heights and before the mesh has been cut to extremely small sizes. But one needs to integrate extremely close to  $t^*$ , if one wishes to really attain the extra few digits, which is only possible when the



computations are well into the asymptotic regime. This is definitely needed in the critical, two-dimensional case, where one wishes to differentiate between several possible proposed formulas for the blow-up as will be seen in section 5.

An example of a typical post-processing operation that is repeatedly performed is the evaluation of quantities of the form  $F(t^* - t)$  for  $t$  extremely close but less than  $t^*$ . In the experiments,  $t^*$  is taken to be the largest value of  $t$  that a particular run can reach beyond which the adaptive mechanism is no longer able to refine the spatial mesh.  $F$  is then evaluated at temporal differences  $t^* - t_i$ ,  $i = 1, 2, \dots$ , where  $t_i$  is the time when the  $i^{\text{th}}$  spatial grid refinement takes place. Since  $t^* - t_i$  can become e.g. of  $O(10^{-20})$ , it is computed as  $\sum_{j=1}^{N_i} k_j n_j$  where  $k_j$  is the size of a temporal step,  $n_j$  is the number of temporal steps of size  $k_j$ , and  $N_i$  is the total number of temporal steps of different size taken between  $t_i$  and  $t^*$ ; the sum is computed from smallest to largest terms. More details on computing particular blow-up rates will be given at the appropriate places in the sequel.

The computations to be reported in the next three sections were performed by a double precision Fortran 77 code that was compiled using the SC1.0 Fortran V1.4 compiler with full optimization on a SparcClassic Sun workstation with 24 MB of RAM running under SunOS 4.1.3. A run (the results of which are reported in Section 5) for the approximation of blow-up in 2 dimensions that started with 1600 spatial mesh intervals initially, and reached a record-high amplitude of  $.985 \times 10^{16}$  after the spatial mesh was refined 50 times, took 9850 total cpu seconds.

#### 4. BLOW-UP: THE THREE-DIMENSIONAL CASE

As was stated in the Introduction, the dynamics of blow-up (collapse) of radially symmetric solutions of the NLS in three dimensions are by now rather well-understood; the reader is referred to the papers [McPSS] and [KSZ] for detailed expositions and further references. In [McPSS] it was concluded that solutions emanating from several initial profiles evolve into a self-similar form which blows up as  $t \uparrow t^*$  according to the law

$$u(r, t) \sim \frac{1}{(t^* - t)^{\frac{1}{2}}} Q \left( \frac{\sqrt{\kappa} r}{(t^* - t)^{\frac{1}{2}}} \right) e^{i\kappa(\ln \frac{1}{t^* - t})}, \quad (4.1)$$

that had been predicted earlier by Zakharov. The complex-valued function  $Q(\xi)$ ,  $\xi \in (0, \infty)$ , and the real number  $\kappa$  solve an 'eigenvalue' problem for a nonlinear ordinary differential equation. The number  $\kappa$  is independent of the initial profile that produced (4.1), and its value is approximately equal to 0.545. The conclusions of [KSZ] are in good agreement with those of [McPSS].

Since the three-dimensional case is under good control, at least as far as the self-similarity of the blow-up and the other features of (4.1) are concerned, it is a good benchmark for a direct integration code such as the one described in this paper. As a test of the code we approximated the blow-up of solutions emanating from a Gaussian (G3) and a 'ring' type (R3) initial profile.

Our first example, labelled G3, corresponds to an initial value  $u^0(r) = 6\sqrt{2}e^{-r^2}$  on  $[0, \infty)$ , restricted to the interval  $[0, R]$  with  $R = 5$ , and scaled to  $[0, 1]$  as

$$v(r) = 6\sqrt{2}e^{-25r^2}, \quad 0 \leq r \leq 1, \quad (4.2)$$

in the notation of (3.1). Hence  $\varepsilon = 1/25$  and the Hamiltonian (3.3) is equal to about  $-0.87783$ . (This example has been considered in [McPSS] and elsewhere. The actual value of the initial



amplitude that we used was 8.485281374.) We approximated the solution using at the beginning a spatial meshlength  $h = 10^{-3}$  (i.e.  $N = 10^3$ ) and a time step equal to  $k = 10^{-4}$ . The number of intervals in the finest mesh region in this and all other experiments in the sequel was taken to be 200. The parameters in the mesh refinement criteria were  $TOL_h = 0.14$  and  $TOL_k = 5 \times 10^{-8}$ . The evolution of the magnitude of the solution is shown in Figures 1a and 1b. The early stages of the development showing the fast collapse at  $r = 0$  appear in Figure 1a, while Figure 1b shows snapshots of later stages. Note that the radial axis, labelled  $x$  in the figure, and the  $|u|$ -axis, labelled  $u$ , are being suitably rescaled in the successive plots of Fig. 1b; the self-similar nature of the singular profile is clearly suggested. By the final, ‘blow-up’ time  $t^* \approx 0.03429946$ , the amplitude at  $r = 0$  had risen to approximately  $.661 \times 10^{12}$  (thus exceeding its initial value by a factor of  $.779 \times 10^{11}$ ), and the code had refined  $NSPLIT = 35$  times the spatial mesh; the final time step used was about  $.847 \times 10^{-25}$ .

We also tried exponentially decaying ‘ring’-type initial profiles that were scaled on  $[0, 1]$  ( $\varepsilon = 1/25$  in (3.1a)) as

$$v(r) = ae^{-br} \left( 1 + br + \frac{b^2 r^2}{2 - bs} \right), \quad 0 \leq r \leq 1, \quad (4.3)$$

having a single maximum at  $r = s$  equal to  $ae^{-bs}(2 + bs)/(2 - bs)$ . We experimented with several values of  $a, b$  and  $s$  and found that the code worked better when  $s$  was small, of course, since in that case enough of the peak is captured in the region of fine grid when the mesh cutting starts. The parameters  $s = 0.06$ ,  $a = 4$ ,  $b = 13$  (giving an initial maximum of 4.178 and  $H(v) = -.15081$ ) correspond to the run that will be referred to henceforth as R3. This ‘ring’ collapsed relatively fast at zero. Using initially  $h = 1/1600$ ,  $k = 10^{-4}$ , and with  $TOL_h = .12$  and  $TOL_k = .5 \times 10^{-6}$ , the code was able to cut the spatial mesh 32 times before stopping at an approximate  $t^* \cong .10145695$ , at which point the amplitude at zero had reached a peak of  $.926 \times 10^{11}$  while the final time step used was about  $.108 \times 10^{-22}$ .

We shall now report on the various blow-up rates that were computed from the output of the runs G3 and R3. The amplitude magnification factors achieved in these examples are considerably larger than the ones previously reported in the literature, and this gives us confidence that the information to be tabulated below is quite accurate. One group of data concerns observed blow-up rates as  $t \rightarrow t^*$ , for several spatial norms of the solution (and the first radial derivative thereof) of (3.1). Let  $A(t)$  be the value at time  $t$  of such a norm of  $u(\cdot, t)$  or  $u_r(\cdot, t)$ . With output generated by the code we calculated  $A(t)$  for  $t$  very close to  $t^*$  and estimated the numbers  $\rho$  such that

$$A(t) \sim (t^* - t)^{-\rho} \text{ as } t \uparrow t^*. \quad (4.4)$$

Specifically, as explained in section 3, we evaluate  $A(t)$  at the instances  $t = t_i$ ,  $i = 1, 2, 3, \dots$ , when the  $i^{\text{th}}$  spatial refinement takes place. Then, approximations  $\rho_i$  to the blow-up rate  $\rho$  of  $A(t)$  are computed in terms of the data at  $t_i$  and  $t_{i+1}$  by the formula

$$\rho_i = -\ln \frac{A(t_i)}{A(t_{i+1})} / \ln \frac{t^* - t_i}{t^* - t_{i+1}}. \quad (4.5)$$

In Table 1 we show the blow-up rates of the  $L^4$  and  $L^\infty$  norm (i.e. of the amplitude) of the solution of (3.1), as well as of the  $L^2$  and  $L^\infty$  of its radial derivative (in the columns labelled  $L_D^2$  and  $L_D^\infty$ ) for the example G3. (Here and in the sequel the  $L^p$ ,  $2 \leq p < \infty$ , norms refer to the quantities  $\left( \int_0^1 |u(r, t)|^p r^{d-1} dr \right)^{\frac{1}{p}}$ . The max norms were calculated over all quadrature points.) The rates are shown at the times  $t_i$  (of the  $i^{\text{th}}$  refinement) for  $i = 10, 11, \dots, 27$ . The



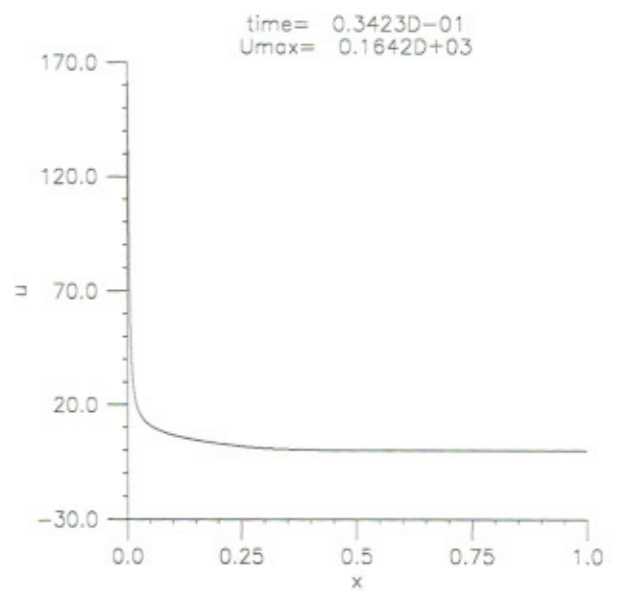
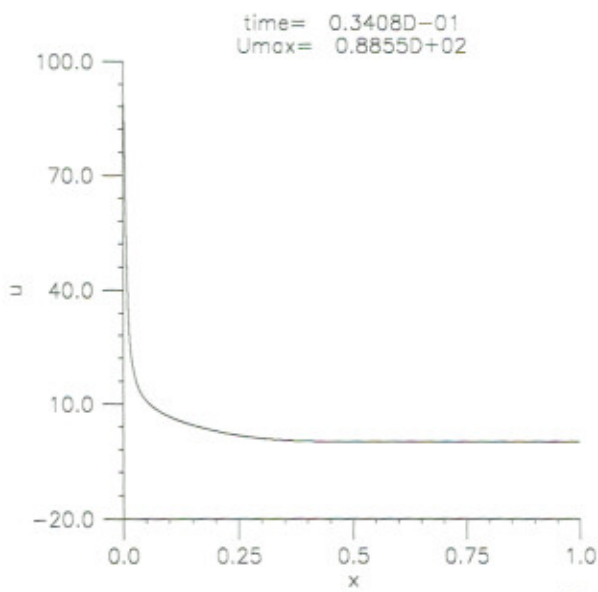
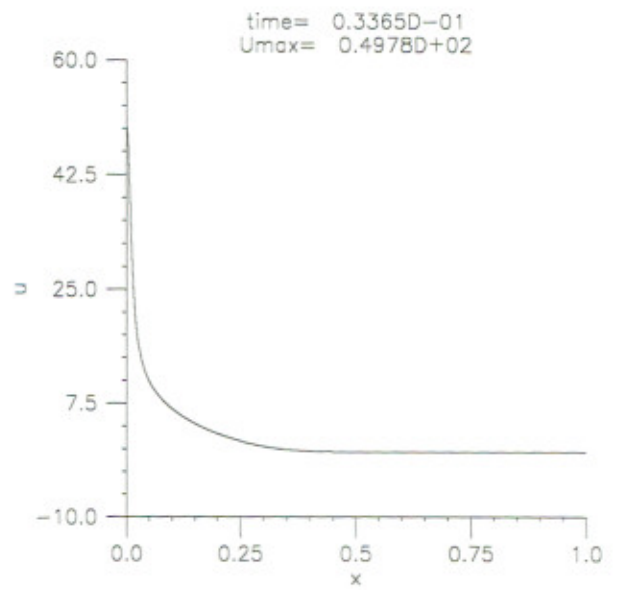
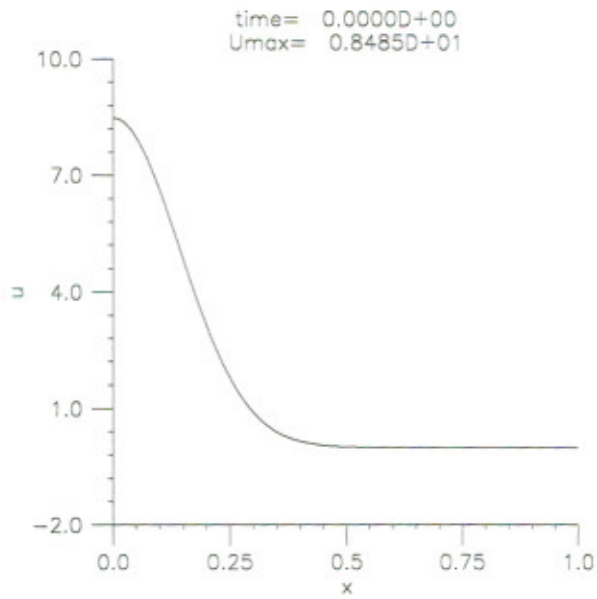


Figure 1a.

Blow-up of the modulus of the solution with Gaussian initial profile G3. Early stages.

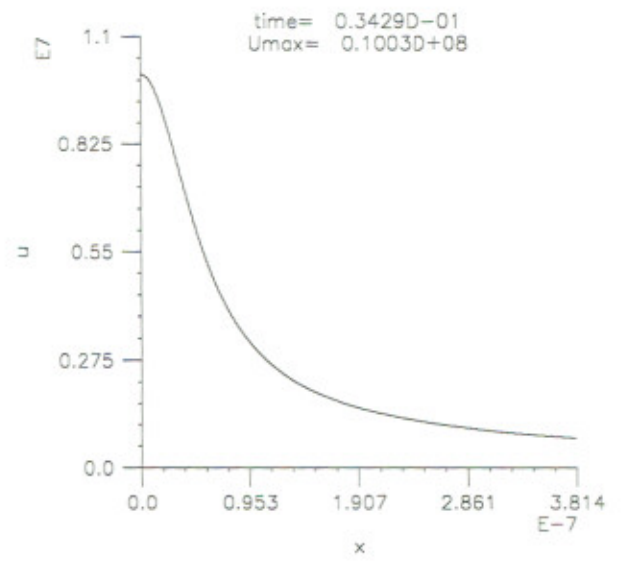
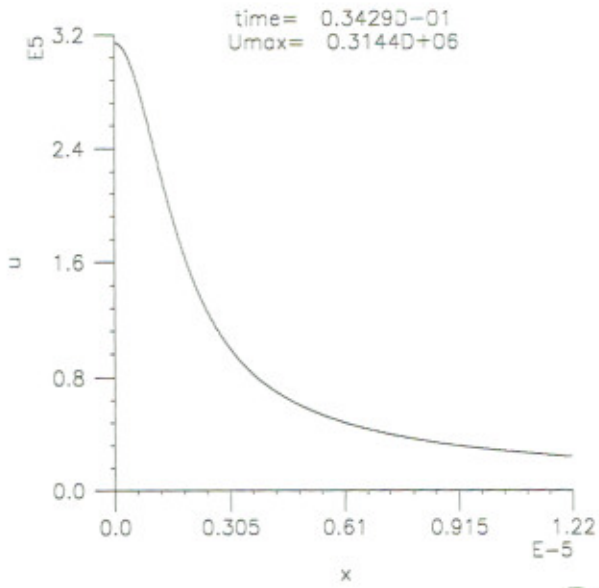
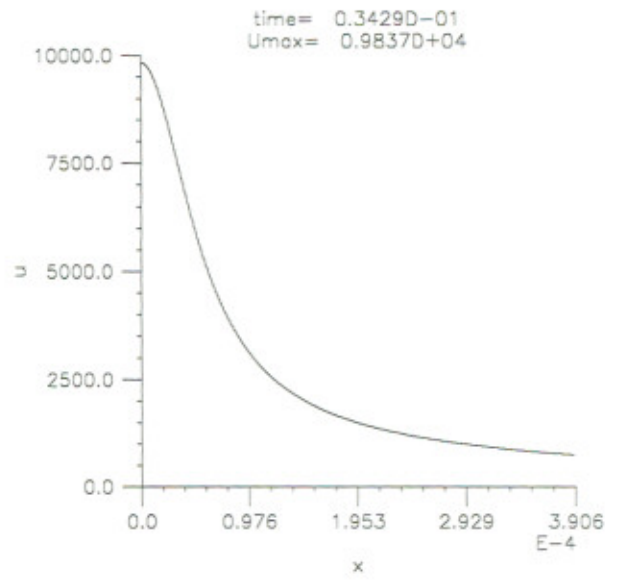
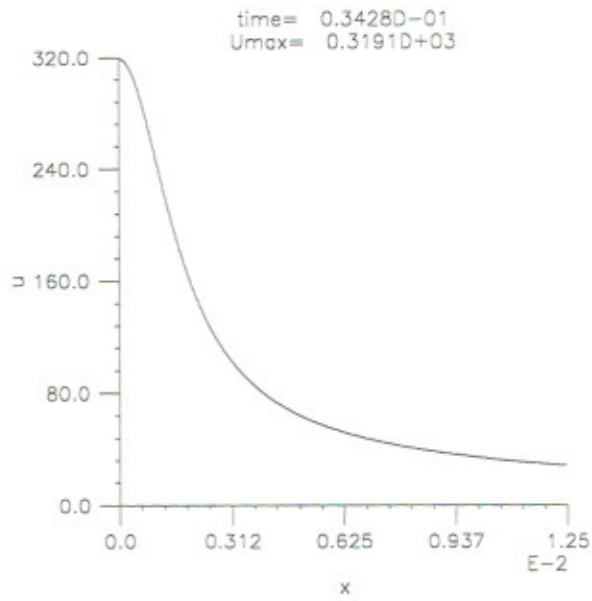


Figure 1b.

Blow-up of the modulus of the solution with Gaussian initial profile G3. Advanced stages.



actual values of  $t_i$  are not shown, being extremely close to  $t^*$ . For  $i \geq 28$ , norm blow-up rate computations are not reliable in this example due to the extreme proximity of  $t_i$  to  $t^*$ .

$i$	$L^4$	$L^\infty$	$L^2_D$	$L^\infty_D$	$\kappa$
10	.12385	.50041	.24827	1.00052	.54528
11	.12438	.49972	.24904	.99966	.54532
12	.12467	.50010	.24948	1.00049	.54525
13	.12482	.50035	.24972	.99983	.54473
14	.12490	.49990	.24984	1.00072	.54518
15	.12495	.49996	.24992	.99956	.54518
16	.12497	.49976	.24996	.99959	.54516
17	.12499	.50007	.24998	1.00024	.54510
18	.12499	.50036	.24999	.99981	.54478
19	.12500	.49964	.24999	1.00079	.54535
20	.12500	.50019	.25000	.99962	.54496
21	.12500	.49986	.25000	.99927	.54495
22	.12500	.50032	.25000	1.00083	.54515
23	.12500	.49985	.25000	1.00009	.54502
24	.12500	.50021	.25000	.99954	.54519
25	.12500	.49965	.25000	1.00067	.54509
26	.12500	.50009	.24999	.99960	.54506
27	.12498	.49994	.24999	.99937	.54485

Table 1  
Blow-up rates, G3

The blow-up rates appear to stabilize quite early in the computation and are quite robust. The law  $(t^* - t)^{-\frac{1}{2}}$  for the amplitude is clearly verified. The  $L^4$  norm of  $u$  and the  $L^2$  and  $L^\infty$  norms of  $u_r$  are shown to blow up at the rates  $\rho = 1/8, 1/4$  and  $1$ , respectively, which are of course consistent with the respective rates that may be computed using formula (4.1).

The last column of Table 1, labelled  $\kappa$ , lists approximations obtained from the data at  $t = t_i$  of the constant  $\kappa$  appearing in the exponential term  $e^{i\kappa \ln \frac{1}{t^* - t}}$  of (4.1). We assumed that the phase of the solution at  $r = 0$  is of the form  $\kappa \ln \frac{1}{t^* - t}$  and computed values of  $\kappa$  at  $t = t_i$  by forming the quotient  $\sigma_i = U(0, t_{i+1})/U(0, t_i)$ , where  $U(0, t_i)$  is the fully discrete approximation produced by the code and evaluated at  $(r, t) = (0, t_i)$ , then computing  $\varphi_i = \arctan(\text{Im}(\sigma_i)/\text{Re}(\sigma_i))$  (or as  $\varphi_i + \pi$  if  $\varphi_i$  is negative) and finally letting

$$\kappa_i = \varphi_i / \ln \frac{t^* - t_i}{t^* - t_{i+1}}. \quad (4.6)$$

The numbers  $\kappa_i$  of the last column of Table 1 show that the phase constant has stabilized and that its value agrees well with the number obtained in [McPSS] and [KSZ].

Table 2 shows the results of the analogous norm blow-up rate calculations as well as the values of  $\kappa$  obtained from the output of the run R3 that corresponds to the ring-type initial profile mentioned previously.

$i$	$L^4$	$L^\infty$	$L_D^2$	$L_D^\infty$	$\kappa$
10	.12469	.50008	.24946	1.00012	.54509
11	.12483	.50007	.24970	1.00007	.54511
12	.12491	.49996	.24983	1.00004	.54503
13	.12495	.50004	.24991	.99999	.54503
14	.12497	.49996	.24995	1.00033	.54500
15	.12499	.50004	.24997	.99962	.54500
16	.12499	.49999	.24999	1.00036	.54507
17	.12500	.49999	.24999	.99970	.54501
18	.12500	.50007	.25000	1.00003	.54499
19	.12500	.49995	.25000	1.00023	.54500
20	.12500	.50001	.25000	1.00005	.54506
21	.12500	.50001	.25000	1.00018	.54502
22	.12500	.49995	.25000	.99994	.54506
23	.12500	.50005	.25000	.99952	.54498
24	.12499	.49996	.24999	1.00034	.54503

Table 2  
Blow-up rates, R3

The rates, that appear to be slightly more robust than those of Table 1, corroborate fully the computational evidence gleaned from the Gaussian initial profile run G3.

## 5. BLOW-UP: THE CRITICAL CASE

In this section we report the results of numerical experiments that we performed with our adaptive code in the critical, two-dimensional case. We focused on computing blow-up rates for the amplitude of the solution of (1.2) at  $r = 0$ , as well as of several of its norms and norms of its radial derivative. As stated in the introduction, we also computed a certain constant occurring in the expression of the phase of the solution at  $r = 0$ , assuming a certain dependence of the phase as a function of  $t$  when  $t$  is close to  $t^*$ , [LPSS]. As in section 4, we experimented with radially exponentially decreasing (Gaussians, rings) initial profiles.

Our first family of examples are Gaussians of various amplitudes. We took, in the notation of (3.1) with  $d = 2$ ,

$$v(r) = A_0 e^{-25r^2}, \quad 0 \leq r \leq 1, \quad (5.1)$$

using the scaling factor  $\varepsilon = 1/25$  and several values of  $A_0$ . We shall label these examples as (G2,  $A_0$ ) in the sequel.

In the case  $A_0 = 6\sqrt{2}$  (actually  $A_0 = 8.485281374$ ), the Hamiltonian (3.3) being equal to about  $-11.520$ , we started with initial mesh sizes  $h = 1/1600$ ,  $k = 0.8 \times 10^{-4}$ . With refinement criteria parameters  $TOL_h = 0.12$  and  $TOL_k = 3 \times 10^{-8}$ , the code was able to perform 34 spatial grid refinements; at the final ('blow-up') time  $t^* = 0.04208980$  it had achieved an amplitude at  $r = 0$  equal to about  $.258 \times 10^{12}$ , the last time step being equal to about  $0.108 \times 10^{-23}$ . The early and later stages of the evolution of the modulus of the solution appear in Figures 2a and b. Output from this run as well as from other similar runs with different initial amplitudes  $A_0$  served to determine the various blow-up rates mentioned above. First, we describe our results on the blow-up rates of the *amplitude*  $A(t)$  of the solution at  $r = 0$ .



It is by now clearly understood (see the discussion and the references quoted in the Introduction), that the amplitude at  $r = 0$  behaves basically like  $(t^* - t)^{-\frac{1}{2}}$  as  $t \uparrow t^*$  but is perturbed (slowed down) by a factor that tends slowly to infinity as  $t \uparrow t^*$ . One may write then that

$$A(t) \sim \left( \frac{F(t^* - t)}{t^* - t} \right)^{\frac{1}{2}} \text{ as } t \uparrow t^*,$$

where the function  $F(s)$ , defined for  $s > 0$ , tends to infinity as  $s \downarrow 0$  slower than any power of  $s$ . As it has been already mentioned in the Introduction, several choices of  $F$  have been made in the literature, e.g.

$$\begin{aligned} F(s) &= \ln \frac{1}{s}, & [\text{VPT}], [\text{Wo}], \\ F(s) &= \left( \ln \frac{1}{s} \right)^\gamma, & 0.35 \leq \gamma \leq 0.65, \quad [\text{KSZ}], \\ F(s) &= \ln \ln \frac{1}{s}, & [\text{LPSS}], [\text{LePSS3}], [\text{Fr}]. \end{aligned}$$

We shall compare these amplitude blow-up laws against numerical results obtained from our adaptive code, including in the comparison the pure power law  $(t^* - t)^{-\frac{1}{2}}$ , i.e. the case  $F(s) = 1$ . Specifically, we shall compute approximations to the power  $\rho > 0$  assuming that the amplitude at  $r = 0$  (i.e.  $\|u(t)\|_\infty$ ) behaves like

$$A(t) \sim [F(t^* - t)/(t^* - t)]^\rho \text{ as } t \uparrow t^*, \quad (5.2)$$

where  $F(s)$ ,  $s > 0$ , is one of the six following laws

$$F(s) = 1, \quad (5.3a)$$

$$F(s) = \ln \frac{1}{s}, \quad (5.3b)$$

$$F(s) = \left( \ln \frac{1}{s} \right)^{0.6}, \quad (5.3c)$$

$$F(s) = \left( \ln \frac{1}{s} \right)^{0.5}, \quad (5.3d)$$

$$F(s) = \left( \ln \frac{1}{s} \right)^{0.4}, \quad (5.3e)$$

$$F(s) = \ln \ln \frac{1}{s}. \quad (5.3f)$$

As in the experiments presented in the previous section, for  $i = 1, 2, 3, \dots$ , we computed  $A_i = A(t_i)$ , the value of  $A$  at the time  $t_i$  of the  $i^{\text{th}}$  spatial refinement, and then calculated approximations  $\rho_i$  of  $\rho$  by the formula

$$\rho_i = \ln \left( \frac{A_i}{A_{i+1}} \right) / \ln \left( \frac{F_i/(t^* - t_i)}{F_{i+1}/(t^* - t_{i+1})} \right), \quad (5.4)$$

where  $F_i = F(t^* - t_i)$ . Table 3 shows  $\rho_i$  for  $14 \leq i \leq 28$  (the quality of the computed  $\rho_i$ 's degenerated for  $i > 28$  due to the extreme proximity of  $t_i$  to  $t^*$ ) with the results for the choices (5.3a-f) for  $F(s)$  appearing in the corresponding columns a-f.

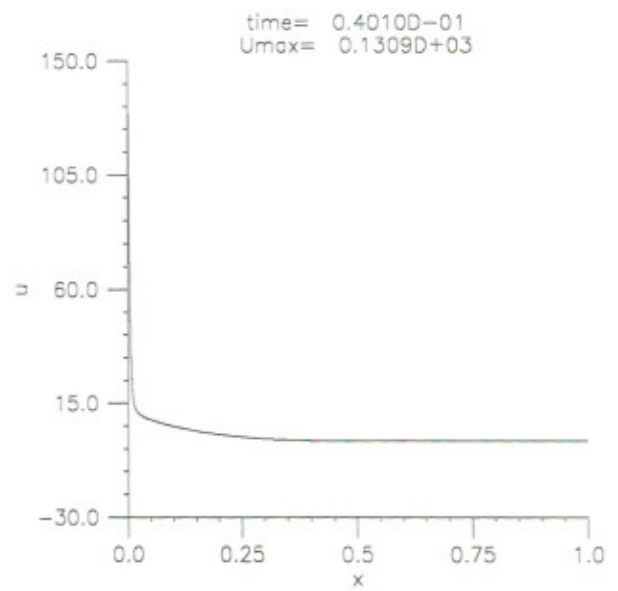
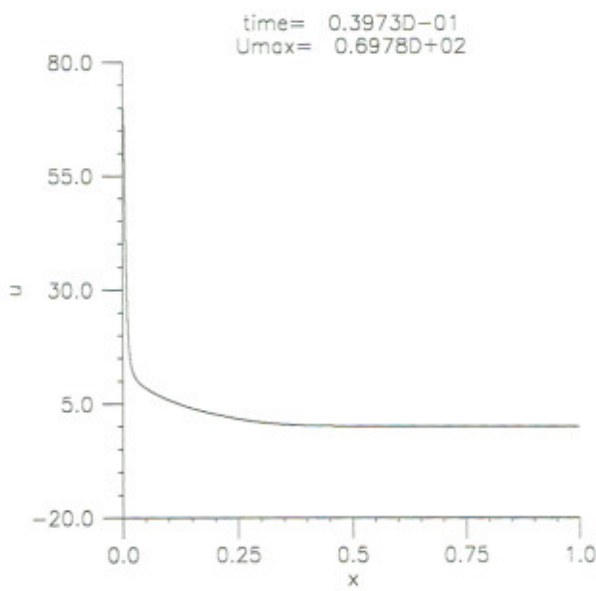
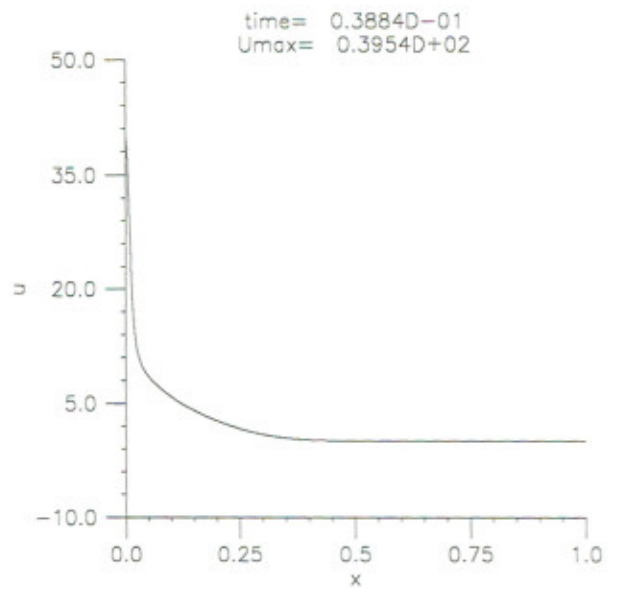
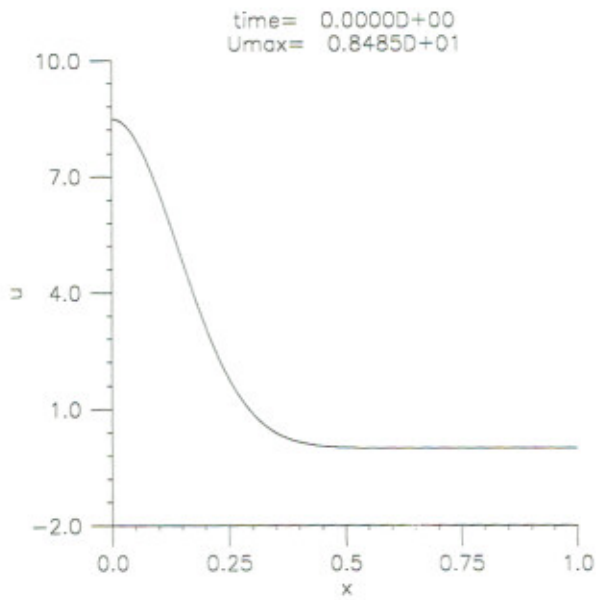


Figure 2a.

Blow-up of the modulus of the solution with Gaussian initial profile  $(G2, 6\sqrt{2})$ . Early stages.



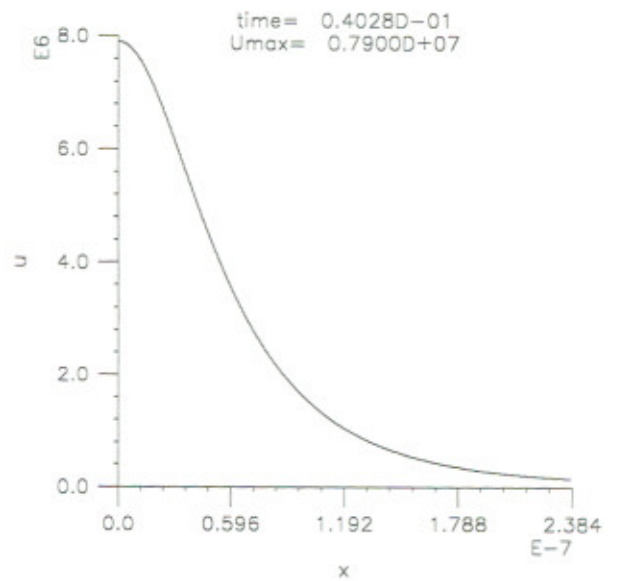
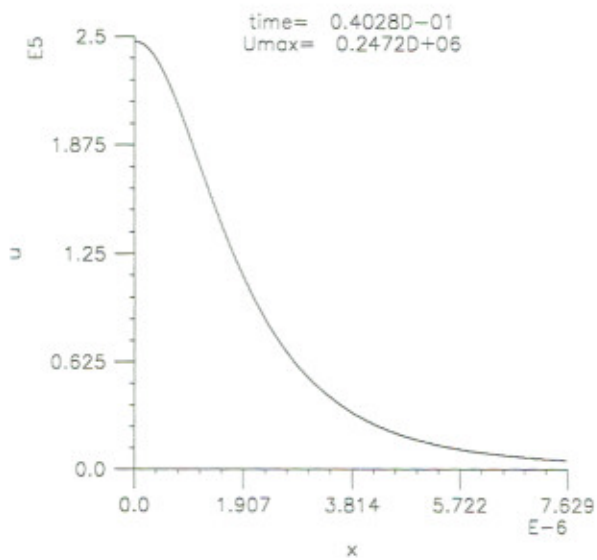
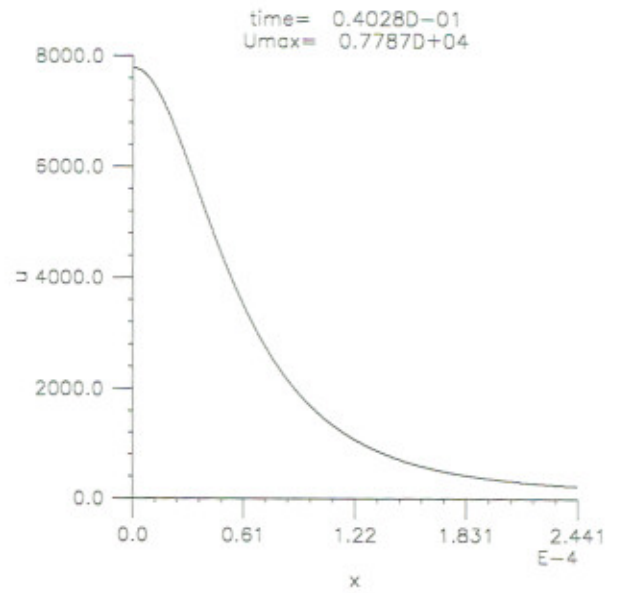
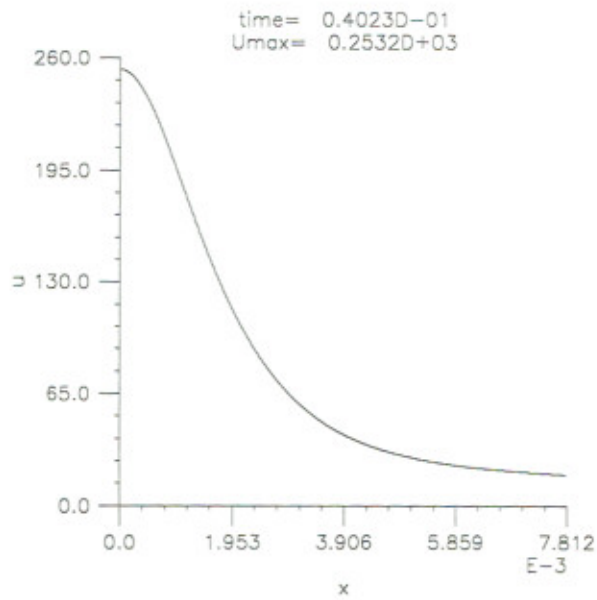


Figure 2b.  
Blow-up of the modulus of the solution with Gaussian initial profile  $(G2, 6\sqrt{2})$ . Later stages.

$i$	a	b	c	d	e	f
14	.50894	.48828	.49634	.49839	.50047	.50222
15	.50756	.48804	.49566	.49761	.49957	.50133
16	.50714	.48860	.49585	.49770	.49956	.50133
17	.50651	.48888	.49579	.49754	.49931	.50108
18	.50600	.48919	.49578	.49746	.49914	.50090
19	.50553	.48947	.49577	.49737	.49898	.50072
20	.50514	.48976	.49580	.49733	.49888	.50060
21	.50479	.49004	.49583	.49730	.49878	.50049
22	.50448	.49030	.49587	.49729	.49871	.50039
23	.50422	.49057	.49594	.49730	.49867	.50033
24	.50396	.49081	.49599	.49730	.49862	.50026
25	.50372	.49103	.49603	.49729	.49856	.50018
26	.50351	.49126	.49609	.49731	.49854	.50013
27	.50323	.49138	.49605	.49723	.49842	.49999
28	.50292	.49145	.49598	.49712	.49827	.49982
Mean [19-28]	.50415	.49061	.49593	.49729	.49864	.50029
Std. dev. [19-28]	.844(-3)	.698(-3)	.110(-3)	.672(-4)	.211(-3)	.276(-3)

Table 3

Blow-up rates of the amplitude  $A(t)$  at  $r = 0$  corresponding to laws (5.3a) - (5.3f). Run with initial profile (G2,  $6\sqrt{2}$ ).

The last two rows of each column of the table show the mean and standard deviation of the rates of that column computed using the values of the data in the window  $i = 19$  to  $i = 28$  closer to the asymptotic regime. (We use the notation  $.844(-3) = .844 \times 10^{-3}$  etc.). As expected, all laws (5.3a) - (5.3f) substituted in (5.2) yield rates close to 0.5. The laws  $a$  and  $b$  are not as stable as the rest. The rates of column  $f$ , corresponding to the log log rate (5.3f) clearly stabilize closer to 0.5 than any other law. The laws  $c$ ,  $d$ , and  $e$ , corresponding to the powers  $\gamma = 0.6, 0.5$  and  $0.4$  give very robust rates which however cluster with small deviation around values that differ from 0.5 by a larger amount as compared to those of the log log case. It is our conclusion that  $F(s)$  given by (5.3f) gives the best fit to the amplitude data generated by the code as  $t$  gets extremely close to  $t^*$ .

This conclusion is reinforced by examining data from other runs corresponding to Gaussian initial profiles of different amplitudes. For example, consider the output from a run labelled (G2, 8) that corresponds to a profile of the form (5.1) with  $A_0 = 8$  (Hamiltonian =  $-8.96$ ). With initial mesh sizes  $h = 1/2400$ ,  $k = 0.75 \times 10^{-4}$  and  $TOL_h = 0.12$ ,  $TOL_k = 3.4 \times 10^{-8}$  the code was able to perform 45 refinements of the spatial grid at which point it reached the final ('blow-up') time  $t^* = .043706879$  achieving a maximum amplitude of about  $.793 \times 10^{15}$ ; the last time step was approximately of size  $.303 \times 10^{-31}$ . With data from this run we generated Table 4, analogous to Table 3.



$i$	a	b	c	d	e	f
18	.50566	.48929	.49571	.49734	.49898	.50073
19	.50524	.48958	.49572	.49728	.49885	.50059
20	.50487	.48986	.49576	.49726	.49876	.50047
21	.50458	.49017	.49583	.49727	.49871	.50041
22	.50427	.49041	.49586	.49724	.49863	.50031
23	.50403	.49068	.49593	.49726	.49860	.50025
24	.50380	.49093	.49600	.49728	.49857	.50020
25	.50360	.49116	.49606	.49730	.49855	.50015
26	.50342	.49140	.49614	.49734	.49854	.50012
27	.50326	.49162	.49621	.49737	.49854	.50010
28	.50309	.49182	.49627	.49739	.49852	.50006
29	.50294	.49201	.49633	.49742	.49851	.50003
30	.50282	.49221	.49640	.49746	.49853	.50001
31	.50269	.49238	.49645	.49748	.49852	.49998
32	.50256	.49254	.49650	.49750	.49851	.49995
Mean [23-32]	.50322	.49168	.49623	.49738	.49854	.50009
Std. dev. [23-32]	.488(-3)	.630(-3)	.196(-3)	.848(-4)	.297(-4)	.971(-4)

Table 4  
Blow-up rates of amplitude  $A(t)$  at  $r = 0$  corresponding to laws (5.3a) - (5.3f). Run with initial profile (G2, 8).

Since the final amplitude reached in this run was higher, we expect rates from data well in the asymptotic regime. The rates of columns a and b improve slightly, while those of columns c, d, e remain basically the same with their counterparts of Table 3. The log log rates  $f$  stabilize further, and are closer to the expected value 0.5, strongly indicating that the correct asymptotic law for the amplitude blow-up is (5.2) with  $F$  given by (5.3f).

As in the three-dimensional case, the code also generates approximations to the blow-up rates of several other norms of the solution and its radial derivative. As an example, in Table 5 we show the temporal blow-up rates of the  $L^3$  and  $L^4$  spatial norms of the solution of (3.1) with initial data (G2, 8) as well as those of the  $L^2$  and  $L^\infty$  norms of its first radial derivatives; the latter appear in the columns labeled  $L_D^2$  and  $L_D^\infty$ . All rates were computed with a log log correction factor: the rates shown are approximations at  $t = t_i$  of positive constants  $\rho$  (computed from values of  $M(t)$  of the corresponding norm produced by the code) assuming that  $M(t) \sim \left[ (\ln \ln \frac{1}{t^* - t}) / (t^* - t) \right]^\rho$ .

$i$	$L^3$	$L^4$	$L_D^2$	$L_\infty^D$
18	.16668	.25023	.50045	1.00123
19	.16666	.25017	.50035	1.00150
20	.16664	.25013	.50026	1.00113
21	.16663	.25010	.50019	1.00048
22	.16662	.25007	.50014	1.00119
23	.16661	.25004	.50009	1.00039
24	.16661	.25002	.50005	1.00032
25	.16660	.25001	.50002	1.00081
26	.16660	.24999	.49999	1.00036
27	.16660	.24998	.49997	1.00025
28	.16659	.24997	.49995	1.00017
29	.16659	.24996	.49993	.99990
30	.16659	.24995	.49991	.99981
31	.16659	.24995	.49989	1.00024
32	.16658	.24993	.49986	.99975

Table 5  
Blow-up rates of various norms, (G2, 8).

Hence, we may conclude with confidence from the results of Table 5 (and similarly robust evidence from the other Gaussian initial profile runs) that the blow-up rates are equal to  $1/6$  for the  $L^3$  and  $1/4$  for the  $L^4$  norm of the solution and equal to  $1/2$  for the  $L^2$  and  $1$  for the  $L^\infty$  norm of the radial derivative. These rates are consistent with the rates expected from the following asymptotic expression for  $u$ , put forth by Landman *et al.* in [LaPSS], and valid for small  $r$  as  $t$  approaches  $t^*$

$$u(r, t) \cong \frac{1}{L(t)} R\left(\frac{r}{L(t)}\right) \exp\left[i\tau(t) - \frac{ir^2}{8(t^* - t)}\right], \quad (5.5)$$

where  $L(t) \sim [\ln \ln \frac{1}{t^* - t} / (t^* - t)]^{-\frac{1}{2}}$ . For characterizations of the function  $R(\xi)$ ,  $\xi \geq 0$ , cf. [LaPSS], [KSZ]. In (5.5) the phase  $\tau$  of the solution at  $r = 0$  blows up as  $t \rightarrow t^*$ . It was argued in [LaPSS] by means of asymptotic techniques that the first-order term in the asymptotic expression of  $\tau(t)$  for  $t$  near  $t^*$  is given by

$$\tau(t) \cong \frac{1}{2\lambda} \ln \frac{1}{t^* - t} \ln \ln \frac{1}{t^* - t}, \quad (5.6)$$

where  $\lambda$  is a constant whose value is predicted to be  $\lambda = 3.14$  in [LaPSS] by means of a limiting argument of descent from the supercritical cases  $d > 2$  that uses asymptotic techniques and the numerical solution of a singularly perturbed nonlinear eigenvalue problem.

In the dynamic rescaling framework of [LaPSS] (and also of other cited papers of the same group), (5.6) is the first-order term in the asymptotic expansion as  $t \uparrow t^*$  of the transformed new temporal variable  $\tau(t)$ , which tends to  $\infty$  as  $t \uparrow t^*$ . The exact formula for  $\tau(t)$  is

$$\tau(t) = \int_0^t \frac{ds}{L^2(s)}, \quad 0 \leq t < t^*. \quad (5.7)$$

(It should be noted that the amplitude of the solution  $u(r, t)$  at  $r = 0$  is proportional to  $1/L(t)$ .) In turn,  $L$  is related to a quantity called  $a(\tau)$  and given by

$$a(\tau) = -\frac{1}{L} \frac{dL}{d\tau}, \quad (5.8)$$



with  $L$  considered as a function of  $\tau$ . In [LaPSS] it is argued that  $a(\tau)$  solves an ordinary differential equation and satisfies, to first-order terms in  $\tau$ ,

$$a(\tau) \cong \frac{\lambda}{\ln \tau} \quad \text{as } \tau \rightarrow \infty. \quad (5.9)$$

(Using (5.9) in (5.8) an asymptotic expression may be found for  $L(\tau)$  valid for large  $\tau$ . Substitution in (5.7) then gives (5.6) to first-order terms.)

To verify computationally (by dynamic rescaling, a byproduct of which are approximations of the values of  $a(\tau)$  for increasing  $\tau$ ) the predicted value  $\lambda = 3.14$ , it was deemed necessary in [LaPSS] to compute  $a(\tau)$  to the next-order term. This expression found was

$$a(\tau) \cong \frac{\lambda}{\ln \tau + 3 \ln \ln \tau}. \quad (5.10)$$

Plotting  $a(\tau)$  vs.  $1/(\ln \tau + 3 \ln \ln \tau)$  Landman *et al.* found that the dependence was indeed linear but that the slope was not equal to  $\lambda = 3.14$  presumably because  $\tau$  was not large enough and the asymptotic regime in which (5.10) is valid had not been reached yet. (See also the relevant comments in [Ma].)

When we tested the form (5.6) versus phase output from our adaptive direct integration code for values of  $t$  close to  $t^*$ , we found that the ratio  $\tau(t)/\ln \frac{1}{t^*-t} \ln \ln \frac{1}{t^*-t}$  did not quite stabilize and took values that were near 0.36, still far from the predicted value  $\frac{1}{6.28} \cong .159$ . At the suggestion of Prof. C. Sulem we tried to compare the computed values of  $\tau(t)$  with an expression that includes the next term in the asymptotic expansion of  $\tau(t)$  as  $t \uparrow t^*$ , corresponding to the level of (5.10). A long computation gave us the next term in the expansion; the corresponding two-term expression for  $\tau(t)$  is

$$\tau(t) \cong \frac{1}{2\lambda} \ln \frac{1}{t^*-t} \left[ \ln \ln \frac{1}{t^*-t} + 4 \ln \ln \ln \frac{1}{t^*-t} \right]. \quad (5.11)$$

This formula was used in our calculations with the objective of recovering the constant  $\frac{1}{2\lambda} =: \kappa$ . Defining, as in the three-dimensional case,  $\varphi_i = \arctan(\text{Im}(\sigma_i)/\text{Re}(\sigma_i))$ , with  $\sigma_i = U(0, t_{i+1})/U(0, t_i)$ , we computed approximations of  $\kappa$  at  $t_i$  by

$$\kappa_i = \varphi_i / \ln \mu_i, \quad (5.12)$$

where  $\mu_i := (t^* - t_i)^{\alpha_i} / (t^* - t_i)^{\alpha_{i+1}}$ ,  $\alpha_i := \ln \ln \frac{1}{t^*-t_i} + 4 \ln \ln \ln \frac{1}{t^*-t_i}$ .

In Table 6 we show the results of three computations of the constant  $\kappa$  (at times  $t_i$  of the  $i^{\text{th}}$  spatial refinement of each run as usual) from three runs, with initial data  $(G2, 6\sqrt{2})$ ,  $(G2, 8)$  and  $(G2, 4)$ , respectively. The parameters of the first two runs have been already specified. The third, corresponding to initial data of the form (5.1) with  $A_0 = 4$  (Hamiltonian =  $-0.32$ ), started with  $h = 1/1600$ ,  $k = 10^{-4}$ , and after performing 50 spatial refinements using  $TOL_h = 0.12$ ,  $TOL_k = 3.2 \times 10^{-8}$  stopped at  $t^* = .14544513$  achieving a maximum amplitude at  $r = 0$  of  $.985 \times 10^{16}$  with a final temporal stepsize of  $.631 \times 10^{-33}$ . In all three examples the phase constant was between .15 and .16 increasing slowly with  $i$  until accuracy was lost when the values of  $t_i$  became extremely close to  $t^*$ . The numbers of the last run seem to be more stable and robust indicating that the asymptotic regime was reached. It is safe then to conclude that our computations verify quite accurately the predicted rate  $\frac{1}{2\lambda} = 0.159$  of Landman *et al.*

(G2, $6\sqrt{2}$ )		(G2, 8)		(G2, 4)	
$i$	$\kappa_i$	$i$	$\kappa_i$	$i$	$\kappa_i$
16	.14701	20	.15146	20	.15574
17	.14807	21	.15215	21	.15619
18	.14903	22	.15279	22	.15662
19	.14990	23	.15338	23	.15702
20	.15070	24	.15394	24	.15740
21	.15144	25	.15445	25	.15776
22	.15212	26	.15494	26	.15810
23	.15275	27	.15540	27	.15842
24	.15333	28	.15584	28	.15874
25	.15388	29	.15624	29	.15904
26	.15438	30	.15664	30	.15932
27	.15483	31	.15700	31	.15960
28	.15522	32	.15735	32	.15986
29	.15538	33	.15766	33	.16012
		34	.15794	34	.16037
		35	.15815	35	.16061
		36	.15824	36	.16085

Table 6

Constant  $\kappa = 1/2\lambda$  in phase formula (5.11),  $d = 2$ . Results from runs (G2,  $6\sqrt{2}$ ), (G2, 8), (G2, 4).

We now turn to reporting the blow-up rates that we obtained by approximating singular radial solutions of the two-dimensional NLS equation that emanate from other types of initial conditions. As in section 4 we tried ring-type initial profiles. In what follows we present the results of a run, henceforth called (R2), corresponding to an initial profile of the type (4.3) ( $d = 2$ ) with parameters  $a = 4$ ,  $b = 10$ ,  $s = 0.1$ , yielding a ring with a peak of initial height 4.41 at  $r = 0.1$  and a Hamiltonian equal to about  $-4.367$ .

The peak of the ring rises as it moves towards  $r = 0$  and then self-focuses fast. With initial  $h = 1/1600$ ,  $k = 10^{-3}$ , the adaptive mechanism was able to cut the spatial mesh 48 times ( $TOL_h = 0.12$ ,  $TOL_k = 5 \times 10^{-7}$ ) before the code quit at  $t^* = 0.18623359$ , at which point the maximum amplitude had risen to about  $.420 \times 10^{16}$  (Last time step =  $.505 \times 10^{-32}$ ). Table 7 gives the observed blow-up rates of the  $L^\infty$ ,  $L^3$  and  $L^4$  norms of the solution and the  $L^2$  and  $L^\infty$  norms of the radial derivative (all were computed with the log log correction) and the approximations  $\kappa_i$  to the constant  $\frac{1}{2\lambda}$  in the phase formula (5.11).



$i$	$L^\infty$	$L^3$	$L^4$	$L_D^2$	$L_D^\infty$	$\kappa_i$
20	.50171	.16699	.25071	.50142	1.00365	.14845
21	.50155	.16696	.25064	.50128	1.00324	.14957
22	.50142	.16693	.25059	.50117	1.00272	.15062
23	.50129	.16691	.25054	.50108	1.00277	.15161
24	.50121	.16690	.25050	.50099	1.00229	.15255
25	.50112	.16689	.25047	.50094	1.00247	.15343
26	.50109	.16688	.25045	.50091	1.00221	.15430
27	.50104	.16688	.25044	.50088	1.00247	.15514
28	.50100	.16688	.25043	.50085	1.00187	.15595
29	.50098	.16688	.25042	.50083	1.00206	.15674
30	.50096	.16688	.25042	.50083	1.00222	.15751
31	.50095	.16688	.25041	.50082	1.00176	.15827
32	.50094	.16688	.25041	.50082	1.00205	.15903
33	.50095	.16689	.25042	.50083	1.00206	.15977
34	.50095	.16690	.25042	.50085	1.00190	.16050

Table 7

Blow-up rates of various norms and phase constant  $\kappa = 1/2\lambda$ , R2.

All rates agree to about three digits with their Gaussian initial profile counterparts of Tables 3-6.

## 6. CONCLUSIONS

In this paper we presented a direct, fully discrete, adaptive Galerkin finite element method for approximating, in two and three space dimensions, singular solutions of the radial NLS that blow up at the origin as the temporal variable  $t$  approaches some finite  $t^*$ . The spatial and temporal mesh refinement adaptive techniques used allowed the numerical solutions to reach record amplitude magnifications at the origin, for  $t$  extremely close to the blow-up time  $t^*$ . On the other hand, the several computed blow-up rates were quite robust, lending support to the conclusion that the method describes accurately the characteristics of the singular solution as it blows up. Specifically, in the three-dimensional case, the numerical results clearly indicate that the amplitude of the solution at the origin blows up at the well-known rate  $(t^* - t)^{-\frac{1}{2}}$ , while in the critical, two-dimensional case they confirm that the amplitude blows up according to the log log law  $[\ln \ln \frac{1}{t^* - t} / (t^* - t)]^{\frac{1}{2}}$  of [LPSS], [LePSS3], [Fr]. In addition, the blow-up of the phase of the singular solution is accurately described in two and three dimensions. (The relevant computational problem in the critical case is quite challenging.)

A natural question in blow-up problems is whether the development of singularities can be prevented by the addition of some suitable dissipative term in the equation. In a companion paper to the one in hand we test the ‘stability’ of the blow-up and the blow-up rates of the singular radial solutions of the NLS in two and three dimensions, when the linear, zeroth-order damping term  $-\delta u$ , where  $\delta$  is a small positive number, is added to the right-hand side of (1.2a). Our conclusion is that damping of small size does not prevent the formation of singularities, even in the critical case, and that, predictably, the blow-up rates are close to their counterparts of the undamped equation. These computational results complement the theory of [Ts], which is valid in the three-dimensional case.

Another problem of major interest is to describe how non-radial solutions of the NLS blow



up, say in two space dimensions. In [LPSSW] the cited dynamic rescaling techniques of the previous papers of that group were extended to the general case of the non-radially symmetric equation. It was demonstrated numerically in [LPSSW] that initial data with a single peak evolves into locally radially symmetric solutions that proceed to blow up, presumably at the critical radial case rates. In this direction, an adaptive code capable of simulating 2-D non-radially symmetric solutions has been recently developed, [KP]. In particular, the code is capable of following multi-peak blow-up. This new code follows spatial and temporal mesh refinement strategies similar to those used in the present work. A more radical departure consists in the use of nonconforming elements in space following a formulation pioneered in [B] and subsequently extended in [BJK] and [KJ]. Experiments conducted so far show that several peaks may blow up simultaneously and confirm the results of [LPSSW] in that the peaks evolve into locally radially symmetric solutions. The outcome of these and other related experiments will be reported shortly.

The computational results reported in this paper and its companions to appear, taken together with similar blow-up computations for the generalized Korteweg–de Vries equation (cf., e.g., [BDKMc]), indicate that suitably adaptive finite element techniques can describe accurately the development of point blow-up singularities of solutions of nonlinear dispersive wave equations. A very interesting but hard problem lies ahead: to understand how such adaptive mesh refinement mechanisms really work, and prove rigorously that they permit discrete solutions to blow up, provided the solution of the p.d.e. does.

**Acknowledgements.** The authors would like to thank Prof. G. Papanicolaou for many lectures and discussions on the blow-up of NLS and comments and suggestions on the material of this paper, and Prof. C. Sulem for her suggestion on computing the phase constant in the critical case.

The research reported in this paper was materially aided by the Institute of Applied and Computational Mathematics of the Research Center of Crete, FO.R.T.H., the Science Alliance of the University of Tennessee, and a joint travel grant of the National Science Foundation, USA, and the General Secretariat of Research and Technology, Greece. To these institutions and agencies the authors express their gratitude.

## References

- [ADK1] G.D. Akrivis, V.A. Dougalis and O.A. Karakashian, “On fully discrete Galerkin methods of second-order temporal accuracy for the nonlinear Schrödinger equation”, *Numer. Math.* **59** (1991), pp. 31–53.
- [ADK2] G. Akrivis, V.A. Dougalis and O.A. Karakashian, “Solving the systems of equations arising in the discretization of some nonlinear p.d.e.’s by implicit Runge-Kutta methods”, *Modél. Math. Anal. Numér.* **31** (1997), pp. 251–288.
- [ADKMc] G.D. Akrivis, V.A. Dougalis, O.A. Karakashian and W.R. McKinney, “Galerkin-finite element methods for the Nonlinear Schrödinger Equation”, in *Advances on Computer Mathematics and its Applications*, ed. by E. Lipitakis, pp. 85–106, World Scientific, Singapore 1993.
- [B] G. Baker, “Finite element methods for elliptic equations using nonconforming elements”, *Math. Comp.* **31** (1977), pp. 45–59.



- [BJK] G.A. Baker, W.N. Jureidini and O.A. Karakashian, "Piecewise solenoidal vector fields and the Stokes problem", *SIAM J. Numer. Anal.* **27** (1990), pp. 1466–1485.
- [BDKMc] J.L. Bona, V.A. Dougalis, O.A. Karakashian, and W.R. McKinney, "Conservative, high-order numerical schemes for the generalized Korteweg–de Vries equation", *Phil. Trans. R. Soc. London A* **351** (1995), pp. 107–164.
- [Bu] J.C. Butcher, *The numerical analysis of ordinary differential equations. Runge-Kutta and general linear methods*, J. Wiley, Chichester 1987.
- [CH] T. Cazenave and A. Haraux, *Introduction aux problèmes d'évolution semi-linéaires*, Mathématiques et Applications No 1, SMAI-Ellipses, Paris 1990.
- [CGT] R.Y. Chiao, E. Garmire and C. Townes, "Self-trapping of optical beams", *Phys. Rev. Lett.* **73** (1964), pp. 479–482.
- [Cr] M. Crouzeix, "Sur l'approximation des équations différentielles opérationnelles linéaires par des méthodes de Runge-Kutta", Thèse, Université Paris VI, 1975.
- [CHS] M. Crouzeix, W.H. Hundsdorfer and M.N. Spijker, "On the existence of solutions to the algebraic equations in implicit Runge-Kutta methods", *BIT* **23** (1983), pp. 84–91.
- [DV] K. Dekker and J.G. Verwer, *Stability of Runge-Kutta methods for stiff nonlinear differential equations*, North-Holland, Amsterdam 1984.
- [ETh] K. Eriksson and V. Thomeé, "Galerkin methods for singular boundary value problems in one space dimension", *Math. Comp.* **42** (1984), pp. 345–367.
- [Fi] G. Fibich, "Self-focusing in the nonlinear Schrödinger equation for ultrashort laser-tissue interactions", Ph.D. Thesis, New York University, New York 1994.
- [FP] G. Fibich and G. Papanicolaou, "Self-focusing in the perturbed and unperturbed nonlinear Schrödinger equation in critical dimension", Preprint 1997.
- [Fr] G.M. Fraiman, "Asymptotic stability of manifold of self-similar solutions in self-focusing", *Soviet Physics JETP* **61** (1985), pp. 228–233.
- [GV] J. Ginibre and G. Velo, "On a class of nonlinear Schrödinger equations I: the Cauchy problem, general case", *J. Funct. Anal.* **32** (1979), pp. 1–32.
- [Gl] R.T. Glassey, "On the blowing up of the solutions in the Cauchy problem for nonlinear Schrödinger equations", *J. Math. Phys.* **18** (1977), pp. 1974–1977.
- [KAD] O. Karakashian, G.D. Akrivis and V.A. Dougalis, "On optimal-order error estimates for the Nonlinear Schrödinger Equation", *SIAM J. Numer. Anal.* **30** (1993), pp. 377–400.
- [KJ] O.A. Karakashian and W.N. Jureidini, "A nonconforming finite element method for the stationary Navier-Stokes equations". *SIAM J. Numer. Anal.* To appear.
- [KP] O.A. Karakashian and M. Plexousakis, "Adaptive methods for nonradially symmetric solutions of the Nonlinear Schrödinger equation". In preparation.

- [Ka] T. Kato, "On nonlinear Schrödinger equations", *Annales Inst. H. Poincaré, Phys. Théor.* **46** (1987), pp. 113–129.
- [KSZ] N.E. Kosmatov, V.F. Shvets and V.E. Zakharov, "Computer simulation of wave collapses in the nonlinear Schrödinger equation", *Physica D* **52** (1991), pp. 16–35.
- [LPSS] M.J. Landman, G.C. Papanicolaou, C. Sulem and P.L. Sulem, "Rate of blowup for solutions of the nonlinear Schrödinger equation at critical dimensions", *Phys. Rev. A* **38** (1988), pp. 3837–3843.
- [LPSSW] M.J. Landman, G.C. Papanicolaou, C. Sulem, P.L. Sulem and X.P. Wang, "Stability of isotropic singularities for the nonlinear Schrödinger equation" *Physica D* **47** (1991), pp. 393–415.
- [LeMPSS] B. Le Mesurier, G. Papanicolaou, C. Sulem and P.-L. Sulem, "The focusing singularity of the nonlinear Schrödinger equation", in *Directions in Partial Differential Equations*, M.G. Crandall, P.H. Rabinowitz and R.E. Turner, eds, pp. 159–201, Academic Press, New York 1987.
- [LePSS2] B.J. Le Mesurier, G. Papanicolaou, C. Sulem, and P.L. Sulem, "Focusing and multifocusing solutions of the nonlinear Schrödinger equation", *Physica D.* **31** (1988), pp. 78–102.
- [LePSS3] B.J. Le Mesurier, G. Papanicolaou, C. Sulem and P.L. Sulem, "Local structure of the self-focusing singularity of the nonlinear Schrödinger equation", *Physica D* **32** (1988), pp. 210–226.
- [Ma] V.M. Malkin, "On the analytical theory for stationary self-focusing of radiation", *Physica D* **64** (1993), pp. 251–266.
- [McPSS] D.W. McLaughlin, G.C. Papanicolaou, C. Sulem, P.L. Sulem, "Focusing singularity of the cubic Schrödinger equation", *Phys. Rev. A* **34** (1986), pp. 1200–1210.
- [Ne] A.C. Newell, *Solitons in Mathematics and Mathematical Physics*, CBMS Applied Mathematics Series v.48, SIAM, Philadelphia 1988.
- [RR] J. Rasmussen and K. Rypdal, "Blow-up in Nonlinear Schrödinger Equations", *Parts I and II, Physica Scripta* **33** (1986), pp. 481–504.
- [SE] R. Schreiber and S.C. Eisenstat, "Finite element methods for spherically symmetric elliptic equations", *SIAM J. Numer. Anal.* **18** (1981), pp. 546–558.
- [SF] A.I. Smirnov and G.M. Fraiman, "The interaction representation in the self-focusing theory", *Physica D* **52** (1991), pp. 2–15.
- [Str] W.A. Strauss, *Nonlinear Wave Equations*, CBMS Regional Conference Series in Mathematics v.73, AMS, Providence 1989.
- [SSP] P.-L. Sulem, C. Sulem and A. Patera, "Numerical simulation of singular solutions to the two-dimensional cubic Schrödinger equation", *Comm. Pure Appl. Math.* **37** (1984), pp. 755–778.
- [Ta] V.I. Talanov, "Self-focusing of wave beams in nonlinear media", *JETP Lett.* **2** (1965), pp. 138–141.



- [TSs] Y. Tourigny and J.M. Sanz-Serna, "The numerical study of blow-up with application to a nonlinear Schrödinger equation", *J. Comp. Phys.* **102** (1992), pp. 407–416.
- [TSsM] Y. Tourigny, J.M. Sanz-Serna and J. Ll. Morris, "Approximation of radial functions by piecewise polynomials on arbitrary grids", *Num. Methods for P.D.E.'s* **7** (1991), pp. 1–8.
- [Ts] M. Tsutsumi, "Nonexistence of global solutions to the Cauchy problem for the damped nonlinear Schrödinger equation", *SIAM J. Math. Anal.* **15** (1984), pp. 357–366.
- [VPT] S.N. Vlasov, L.V. Piskunova and V.I. Talanov, "Structure of the field near a singularity arising from self-focusing in a cubically nonlinear medium", *Soviet Physics JETP* **48** (1978), pp. 808–812.
- [We] M.I. Weinstein, "Nonlinear Schrödinger equation and sharp interpolation estimates", *Communs. in Math. Phys.* **87** (1983), pp. 567–576.
- [Wo] D. Wood, "The self-focusing singularity in the nonlinear Schrödinger equation," *Studies in Appl. Math.* **71** (1984), pp. 103–115.
- [Za] V.E. Zakharov, "Collapse of Langmuir waves", *JETP* **35** (1972), pp. 908–922.
- [ZS] V.E. Zakharov and V.S. Synakh, "The nature of the self-focusing singularity", *Soviet Physics JETP* **41** (1976), pp. 465–468.